IEEE Access
Multidisciplinary | Rapid Review | Open Access Journal

Date of publication xxxx 00, 0000, date of current version xxxx 00, 0000.

Digital Object Identifier 10.1109/ACCESS.2024.0429000

The Unified Synthesis of Flat-Beam Multi-Directional Metasurface Rectennas: A Review for Pervasive Wireless Power Beyond Directional Limits

ATHUL PARAMESWARAN[1,1], MANOJ KUMAR[2, 1], (Member, IEEE), BASUDEV MAJUMDER[1,2], (Member, IEEE), IGNACIO GARCIA ZUAZOLA[3,3], (Senior Member, IEEE), MD JALEEL AKHTAR[2,3], (Fellow, IEEE), MANISH KUMAR[4,4], (Member, IEEE)

[1]Indian Institute of Space Science and Technology, Thiruvananthapuram, Kerala, India
[2]Department of Electrical Engineering, Indian Institute of Technology, Kanpur, India
[3]School of Computing and Digital Media, London Metropolitan University, London, United Kingdom
[4]Department of Electronics Engineering, Zakir Husain College, Delhi University, Delhi, India

Corresponding author: Manoj Kumar.

This work was supported by the Department of Science & Technology, Government of India, Project No. DST/EE/2025226.''

ABSTRACT Battery-free Internet of Things (IoT) systems require wireless power transfer (WPT) receivers that are robust to variations in orientation and polarization. Conventional rectennas, however, exhibit strong directional sensitivity and limited adaptability, which constrains their practical deployment. This review presents a unified synthesis of three emerging rectenna architectures developed to mitigate angular misalignment, flat-beam rectennas, multidirectional rectennas, and metasurface-assisted lens rectennas. A comparative taxonomy is developed to systematically evaluate these approaches in terms of angular coverage, RF–DC conversion efficiency ($\eta_{\mathrm{RF\text{-}DC}}$), implementation complexity, and scalability. Beyond summarizing recent advances, this paper analyzes persistent research gaps common to all techniques, including narrowband operation, limited system-level validation, and manufacturing constraints. A decision-oriented framework is further proposed to guide architecture selection for application-specific scenarios, such as mobile, wearable, and fixed IoT deployments. Convergent future research directions are outlined, including adaptive and broadband designs, multifunctional integration, and emerging concepts such as dynamic metasurfaces, to support the development of pervasive, orientation-independent wireless power solutions for next-generation IoT networks.

INDEX TERMS Ambient Energy Scavenging, Angular Misalignment, Flat-beam Rectennas, Gradient-Index Metasurface, Internet of Things (IoT), Multidirectional Rectennas, Orientation-Independent Energy Harvesting

I. INTRODUCTION

THE Internet of Things (IoT) is transforming modern infrastructure, enabling smart industrial systems [1], healthcare monitoring [2], and intelligent transportation networks [3]. However, the widespread deployment of IoT nodes faces an energy constraint, their reliance on conventional chemical batteries with finite lifespans, maintenance requirements, and scalability limitations [4]–[7]. Wireless power transfer (WPT) presents a compelling alternative, offering potential for continuous, cable-free energy delivery to distributed electronic devices. WPT systems are categorized into near-field and far-field approaches. Near-field WPT, operating through inductive or capacitive coupling, provides short-range power delivery but suffers from sensitivity to spatial misalignments between transmitter and receiver [8]–[10]. These misalignments degrade mutual coupling, detune resonant frequencies, and can create safety hazards through stray field heating [11], [12]. Far-field WPT, conversely, utilizes propagating electromagnetic waves and includes two distinct approaches dedicated radio-frequency WPT (RF-WPT) em-

ploying controlled power beams, and ambient RF energy harvesting (RFEH) that harvests energy from existing broadcast signals such as television, cellular, and Wi-Fi transmissions [13]. RFEH systems operate at ultra-low power densities, constrained by the sparse and unpredictable nature of ambient RF environments. The performance of far-field WPT systems is quantified through power conversion efficiency (PCE) and RF-to-DC efficiency ($\eta_{\text{RF-DC}}$). PCE represents the end-to-end efficiency from transmitted RF power to delivered DC power, including propagation, matching, polarization, and rectification losses [14], [15]. $\eta_{\text{RF-DC}}$ denotes the rectifier conversion efficiency and depends on the input power level, impedance matching conditions, diode characteristics, and load requirements.

A key challenge in far-field WPT is angular and spatial misalignment between transmitters and receivers. Even minor orientation changes can degrade received power and system efficiency [16]. This problem is exacerbated in dynamic environments where IoT devices may be mobile or arbitrarily oriented, such as wearable electronics, sensors on rotating machinery, or autonomous drones. Therefore, maintaining rectenna efficiency over a range of incidence angles is necessary for battery-free IoT operation.

Although several reviews cover rectenna technology [17]–[21], a systematic comparison of flat-beam, multidirectional, and lens-assisted architectures aimed at mitigating angular misalignment is still missing. This review synthesizes and compares contributions from over twenty research groups addressing angular misalignment in far-field wireless power transfer through flat-beam, multidirectional, and lens-based rectenna architectures. The main contributions of this work are summarized as follows:

1) We introduce a unified taxonomy that compares flat-beam, multidirectional, and lens-assisted rectenna architectures with respect to angular coverage, $\eta_{\text{RF-DC}}$, implementation complexity, operating frequency, and scalability.
2) We identify research gaps common to all architectures, including limited system-level demonstrations, narrowband operation, scalability and manufacturing challenges, and the absence of standardized performance benchmarks.
3) We present a decision-oriented framework that links rectenna architecture selection to deployment scenarios, highlighting key performance and implementation trade-offs for practical wireless power harvesting applications.

The paper is organized as follows. Section II presents a taxonomy of angular misalignment mitigation strategies. Section III reviews ambient RF energy measurements. Sections IV-VI detail flat-beam, multidirectional, and metasurface-assisted lens rectennas, respectively. Section VII provides comparative analysis and future directions, with conclusions in Section VIII.

II. TAXONOMY OF ANGULAR MISALIGNMENT MITIGATION STRATEGIES

The design of far-field WPT systems involves a trade-off between directive gain and angular coverage. Conventional rectennas are optimized for peak $\eta_{\text{RF-DC}}$ under boresight alignment, but their performance degrades rapidly under angular or lateral misalignment, limiting practical deployment in mobile or arbitrarily oriented devices. To address this limitation, three architectural paradigms have emerged, each using distinct physical mechanisms to improve robustness against misalignment.

Flat-beam rectennas reduce sensitivity to lateral misalignment through a flattened radiation pattern that sustains consistent gain across a wide region. While flat beams support lateral displacement, they accommodate angular variation in sectorized arrangements. Conventional arrays rely on amplitude tapering to concentrate energy near broadside [22], [23], whereas flat-beam designs redistribute gain to form a flat-top profile, trading peak directivity for increased tolerance to displacement and orientation. Each rectifying element in an array receives equal incident power when illuminated with a flat-beam transmitter [24]–[27]. This architecture suits scenarios where devices remain within known spatial limits while their exact position or orientation varies.

Multidirectional rectennas achieve wide angular coverage through spatial diversity. They employ multiple discrete antenna elements oriented in different directions. This approach differs from flat-beam designs by using separate receiving apertures rather than modifying a single aperture's radiation pattern. Energy collected from spatially distributed elements combines through three main approaches. RF combining merges antenna outputs prior to rectification. DC combining connects each element to an individual rectifier, with the DC outputs summed in series or parallel configurations [28]. Hybrid RF/DC combining groups elements at the RF stage and merges the resulting outputs at the DC stage [29]. Recent advances extend coverage from azimuthal patterns to three-dimensional spherical coverage through arrangements of end-fire and boresight elements [30]–[32].

Metasurface-assisted lens rectennas use engineered structures to shape incident wavefronts and direct energy toward designated rectifying elements. Typical implementations employ gradient-index lenses, including Luneburg or Rotman lenses, or custom metasurfaces [39] to focus incident energy from multiple angles onto designated focal points. This architecture supports high gain along several predetermined directions without active beamforming, maintains fully passive operation, enables custom frequency responses through metasurface design, and offers compact integration despite its multi-beam capability. The design shifts complexity from electronic combining networks into the physical geometry of the lens or metasurface. Such systems are well suited for mmWave WPT, where small apertures achieve high directivity and regulations permit elevated effective isotropic radiated power [40]. Target applications include powering 5G IoT nodes and supplying energy to multiple spatially separated

TABLE 1. Measured ambient RF strength in different countries, where S denotes the RF power flux density and P_{RF} denotes the received power.

Montreal (Canada) [33]								
Frequency (MHz)	DTV	LTE700	GSM/LTE850	LTE1700/2100	LTE1900	Wi-Fi	LTE2600	
Metro P_{RF} (dBm) at Stations	-66.27 to -19.97	-63.91 to -19.08	-60.86 to -19.73	-65.79 to -27.11	-63.13 to -20.16	-72.98 to -58.25	-78.89 to -34.34	
Residential P_{RF} (dBm) at Areas	-68.12 to -25.97	-58.72 to -37.38	-62.22 to -41.62	-62.94 to -44.17	-66.09 to -42.95	-74.53 to -59.80	-75.86 to -54.26	
Singapore [34]								
Frequency (MHz)	925-960		1805-1880			2110-2170		
S (nW/cm^2)	2.38-25.672		14.39-156			19.66-207.92		
Greater London (UK) [35]								
Frequency (MHz)	470-610	880-915	925-960	1710-1785	1805-1880	1920-1980	2110-2170	2400-2500
S (nW/cm^2)	460	39	1930	20	6390	66	240	6
Liverpool (UK) [36]								
Frequency (MHz)	1200-4800 (outdoor)				1200-4800 (indoor)			
S (nW/cm^2)	-10 to 31.6				-0.1 to 0.316			
Metropolitan Areas of Melbourne (Australia) [37]								
Frequency (MHz)	50	100	200	500	800	1000	2000	3000
P_{RF} (dBm) RMIT	-37	3	-29	5	-10	-20	-27	-67
P_{RF} (dBm) Inner City	-67	-13	-25	-19	-35	-27	-29	-67
Mount P_{RF} (dBm) at Dandenong	-10	-7	-29	-7	-40	-38	-34	-67
Hong Kong [38]								
Frequency (MHz)	930-960 (outdoor)		930-960 (indoor)		2110.3-2169.7 (outdoor)		2110.3-2169.7 (indoor)	
S (nW/cm^2)	134		6.85		74.4		4.03	

devices with varying orientations.

These paradigms reflect different trade-offs in gain, angular tolerance, structural complexity, and power-combining efficiency. Flat-beam rectennas stabilize performance against lateral displacement and, when implemented in sectorized configurations, extend tolerance to moderate angular variation. Multidirectional rectennas provide wide angular coverage through spatial diversity, using multiple oriented apertures rather than reshaping the radiation pattern of a single element. Metasurface-assisted lens rectennas achieve high-gain reception from predefined directions through passive wavefront shaping using gradient-index lenses or engineered metasurfaces. Together, these approaches form the basis for the comparative analysis presented in the following sections.

III. THE RFEH ENVIRONMENT

The practical viability of ambient RFEH systems depends on the electromagnetic energy available in real environments, which often remains low and varies with time. Ambient emissions originate from communication services, broadcast stations, and incidental electronic sources, and their strength changes with transmitter activity and spatial distribution [41]. The received power level is influenced through distance to active transmitters, operating frequency, traffic variations, propagation losses from buildings and clutter, and regional limits on effective isotropic radiated power.

Various ambient RF measurement surveys across different continents reveal variation in received power P_{RF} and power flux density S. These measurements show location- and frequency-dependent variation in the ambient RF environment, as summarized in Table 1. In Montreal, Canada, broadband measurements across cellular and broadcast services show large differences between metro stations and residential areas [33]. At metro stations, received power ranges from $-79\,\mathrm{dBm}$ in the LTE2600 band to $-19\,\mathrm{dBm}$ in digital television and cellular bands. Residential areas show lower values that fall between $-76\,\mathrm{dBm}$ and $-26\,\mathrm{dBm}$ across the same bands. These results indicate that transportation hubs with dense transmitter activity offer more suitable conditions for ambient RFEH than suburban regions. In Singapore, measurements taken 150 m from a base station report power flux densities of 2.38 to $25.672\ \mathrm{nW\,cm^{-2}}$ in the 925-960 MHz band, 14.39 to $156\ \mathrm{nW\,cm^{-2}}$ in the 1805-1880 MHz band, and 19.66 to $207.92\ \mathrm{nW\,cm^{-2}}$ in the 2110-2170 MHz band [34]. These strong levels reflect dense urban infrastructure. A large scale survey in Greater London mapped RF activity across 470-2500 MHz [35]. The maximum emissions occurred near 1.8 GHz with peak flux densities of $6390\ \mathrm{nW\,cm^{-2}}$. Other active bands included 470-610 MHz and 925-960 MHz with measured levels of 460 and $1930\ \mathrm{nW\,cm^{-2}}$. Indoor and outdoor measurements in Liverpool show strong attenuation indoors. Outdoor power density ranged from 10 to $31.6\,\mathrm{nW\,cm^{-2}}$, while indoor levels fell to 0.1 to $0.316\ \mathrm{nW\,cm^{-2}}$ [36].

In Melbourne, Australia, received power measurements across $50 - 3000$ MHz show large differences between locations [37]. At the RMIT campus, received power reaches $5\,\mathrm{dBm}$ in the 500 MHz band, while the inner city and the suburban Mount Dandenong sites show weaker and more variable levels that often fall below $-20\,\mathrm{dBm}$ in many bands. Measurements in Hong Kong show strong urban cellular activity in the 930-960 MHz and 2110-2169 MHz bands. Outdoor flux densities reach $134\,\mathrm{nW\,cm^{-2}}$ at 950 MHz and $74.4\,\mathrm{nW\,cm^{-2}}$ in the 2.1 GHz band, while indoor levels fall to $6.85\,\mathrm{nW\,cm^{-2}}$ and $4.03\,\mathrm{nW\,cm^{-2}}$ [38].

These studies show that ambient RF power density ranges from sub-nW/cm^2 indoors to several thousand nW/cm^2 in dense outdoor cellular environments. Cellular communication bands, around 900 MHz and 1.8 GHz, provide the

TABLE 2. Typical Environmental RF Power Density Ranges and Architectural Implications

Power Density Range	Typical Environment	Architectural Suitability	Expected DC Output and Application Viability
0.1-10 nW/cm^2	Indoor residential; rural outdoor	All architectures marginal	Nano-watt level DC output. Suitable only for ultra-low-power wake-up circuits or heavily duty-cycled operation. Requires high rectifier sensitivity.
10-100 nW/cm^2	Urban indoor; suburban outdoor	Multidirectional rectennas preferred	Low micro-watt DC output. Suitable for intermittent sensing with energy storage. Flat-beam rectennas may operate with sufficiently large apertures.
100-1000 nW/cm^2	Dense urban outdoor; proximity to base stations	Flat-beam and multidirectional rectennas viable	Tens of micro-watts DC output. Enables continuous operation of simple sensor nodes. Lens-based rectennas may operate at sub-6 GHz with large apertures.
1-10 μW/cm^2	Very close to transmitters; industrial environments	All architectures potentially viable	Hundreds of micro-watts to low milli-watt DC output. Supports more complex IoT nodes. Lens-based rectennas become practical.
$>$10 μW/cm^2	Millimeter-wave hotspots; dedicated WPT scenarios	Lens-based rectennas most effective	Milli-watt level DC output. Suitable for wearable devices, sensor clusters, and high-efficiency millimeter-wave energy harvesting.

strongest and most stable power sources [33]–[35]. However, the low absolute power levels, combined with large spatial variation, continue to pose two fundamental challenges for RFEH system designs, (i) the power levels are low, often near or below the sensitivity thresholds of practical rectifier circuits; and (ii) the power availability varies with location, making energy delivery difficult without adaptive system designs. The power densities reported in Table 1 impose strict constraints on practical RF energy harvesting. For a typical rectenna, the captured RF power is

$$P_{\mathrm{RF}} = S \times A_{\mathrm{eff}},$$

where S is the incident power density and the effective aperture is approximated by

$$A_{\mathrm{eff}} \approx \frac{\lambda^2}{4\pi}.$$

At 900 MHz ($\lambda \approx 0.33$ m), $A_{\mathrm{eff}} \approx 0.0087$ m^2, meaning that at a relatively high ambient density of 1000 nW/cm^2 (1 μW/cm^2), only ≈ 87 μW of RF power is available at the rectifier input. After antenna losses, impedance mismatch, and rectifier conversion efficiency (10-60% in the -20 to -10 dBm range), the delivered DC power drops to the nano-watt to low-micro-watt regime. This severely limits powered device capabilities, requiring ultra-low-power electronics, duty cycling, and efficient energy storage. Nevertheless, ambient RF remains a viable energy source for ultra-low-power applications (e.g., sensor nodes, RFID-scale devices, wearables in dense urban settings), provided that harvesting systems offer

- angular tolerance for unknown incidence directions,
- multi-band or wideband operation,
- adaptive matching and rectifier topologies for fluctuating input conditions.

To contextualize these values for system design, ambient RF power density ranges and their architectural implications are summarized in Table 2. Most ambient environments (indoor to typical urban outdoor) fall below 1 μW/cm^2, placing severe constraints on harvested power. In these low-density regimes (<100 nW/cm^2), multidirectional architectures that maximize aperture utilization through spatial diversity are generally most viable. As power density increases toward dedicated WPT scenarios ($>$1 μW/cm^2), the efficiency advantages of flat-beam and lens-based architectures become more significant, at millimeter-wave frequencies where regulatory limits permit higher transmitted power. This framework clarifies why angularly robust designs must simultaneously address both low absolute power and directional uncertainty to be practically useful across real-world environments.

IV. FLAT-BEAM RECTENNAS

Flat beam rectennas form a class of receiver structures that establish a broad region of near uniform gain rather than a single dominant reception direction. The aim is to sustain similar incident power levels across the receiving aperture when the source is displaced laterally or when moderate angular variation occurs. This is achieved through controlled shaping of the array excitation and element arrangement, which produces a flattened pattern in place of a narrow peak. Conventional arrays using amplitude tapering prioritize high broadside directivity [22], [23], whereas flat-beam configurations trade peak gain for stable reception over a wider spatial region. The resulting pattern reduces sensitivity to small changes in position or orientation and supports predictable performance within the intended operating bounds. This section outlines the design methods, representative implementations, and measured behaviour of flat beam rectennas.

A. DESIGN PRINCIPLES AND OPERATIONAL MECHANISMS

The design objective for flat-beam rectennas is to achieve equal incident power density at each rectifying element when illuminated from directions within the target angular sector.

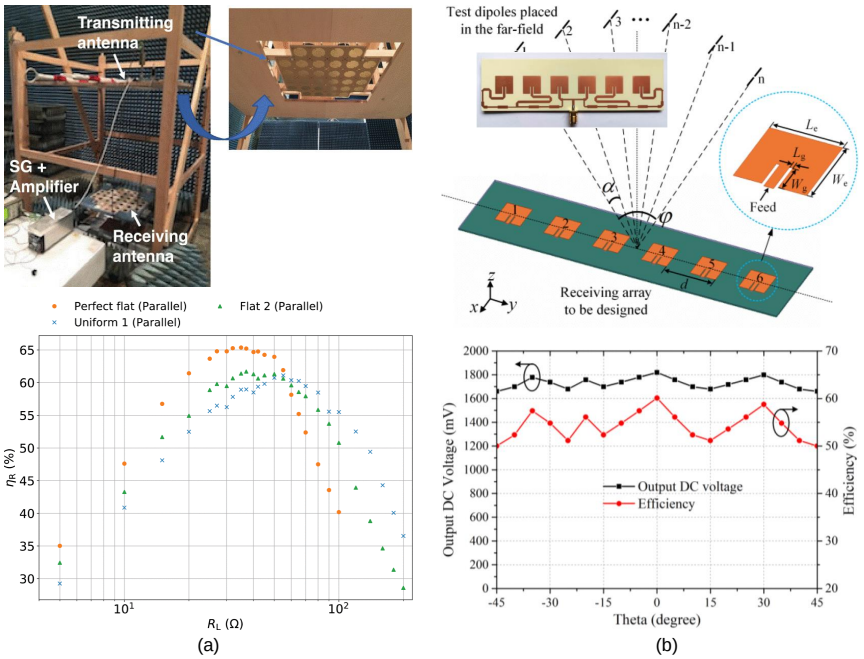

FIGURE 1. Representative flat-beam rectenna designs: (a) 32-element transmitter and 37-element rectenna system [42]; (b) Six-element QCQP-optimized array [43].

TABLE 3. Performance Comparison of Flat-Beam Rectennas Under Different Illumination Conditions

Parameter	Flat-beam Tx + Flat-beam Rx	Narrow-beam Tx + Flat-beam Rx
Incident Power Distribution	Uniform across array	Localized hotspot
DC Output Characteristics	Uniform voltage across elements	Highly non-uniform; only illuminated elements produce significant output
Angular Stability	Stable within designed angular range	Highly sensitive to alignment
Total Harvested Power	Stable and scalable with array size	Fluctuates with beam position
Misalignment Tolerance	Good lateral and angular tolerance	Poor tolerance; requires precise alignment
Effective System Behavior	True orientation-independent harvesting	Scanning array with directional sensitivity
Ideal Application Scenario	Mobile/IoT devices with random orientation	Fixed point-to-point power transfer

This is accomplished through control of the array excitation coefficients, element spacing, and sometimes element geometry. The operational principle can be understood through two complementary perspectives such as joint transmitter-receiver flat-beam systems and flat-beam receiver with conventional transmitter. In ideal scenarios where both transmitter and receiver employ flat-beam designs, the system yields a uniform power density distribution across the receiving array for all angles within the designed coverage sector [42]. Each rectifying element receives similar RF power, and generates similar DC output voltage. The total harvested power scales linearly with the number of active elements, providing stable power delivery despite angular variations. In more practical scenarios where the transmitter employs a conventional narrow beam, the flat-beam rectenna exhibits a scanning behavior. The incident RF power forms a ''hotspot'' that moves across the array as the angle of arrival changes. Crucially, each rectifying element is designed to have nearly identical power conversion characteristics. Therefore, whichever element is illuminated at the center of the hotspot generates consistent DC output. As the angle varies and the hotspot scans across different elements, the total combined DC output remains stable provided the transmitter's beamwidth illuminates a sufficient number of elements at any given angle.

B. IMPLEMENTATION TECHNIQUES

A range of implementation strategies have been developed to realise flat-beam patterns, including excitation optimisation, quadratic constrained quadratic programming (QCQP), sequential feeding, and structural modifications to antenna elements. These methods differ in complexity and scalability but share the objective of producing a broadened and stable gain profile across the desired angular region. One of the earliest full-system demonstrations appears in Fig. 1(a), which shows a 32-element microstrip patch transmitter and a 37-element rectenna array designed for uniform coverage [42]. The system achieved an analytical and simulated $\eta_{\mathrm{RF\text{-}DC}}$ of 80%, with measured efficiencies of 65.4% (parallel) and 68.5% (series). The observed efficiency loss was largely due to reduced aperture efficiency and axial-ratio mismatch, which lowered the connection efficiency η_c. A sequential array architecture was then employed to suppress mutual

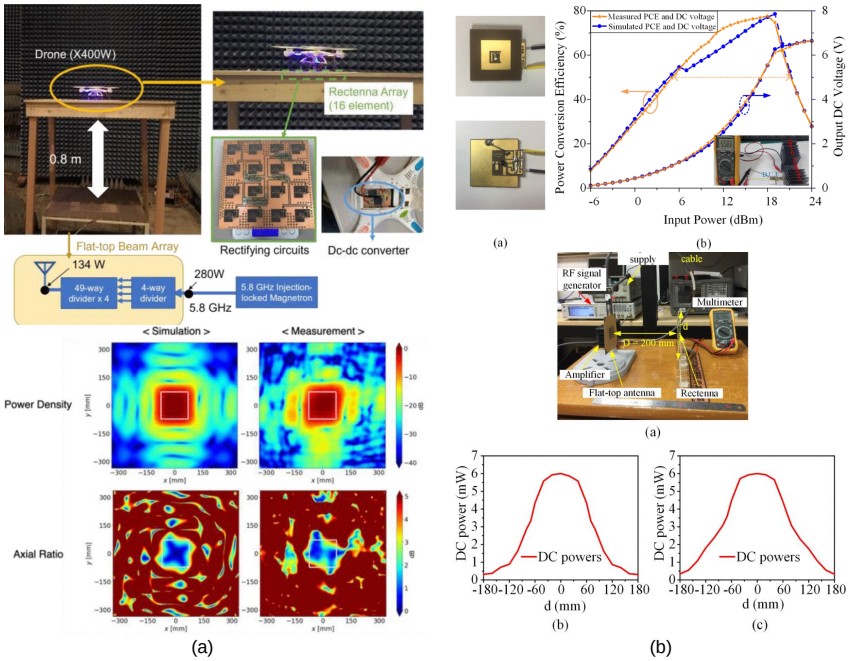

FIGURE 2. **(a) 196-sequentially-fed flat-beam array [44]; (b) Low-profile aperture-coupled patch antenna featuring a mushroom structure [45].**

coupling and reflections at the receiving plane, producing a more uniform flat-beam response and improving wide-angle reception. Earlier work also demonstrated that non-uniform excitation can enhance beamwidth without severely compromising efficiency. A 1×4 patch array with optimised excitation achieved a twofold increase in H-plane beamwidth compared to a uniformly excited array, maintaining $\eta_{\text{RF-DC}}$ above 50% for incidence angles between -38° and $+35^\circ$ [46]. This result demonstrates the feasibility of jointly optimizing antenna beamwidth and rectifier performance for wide-angle RF energy harvesting. Advanced optimisation approaches have since been adopted to enable control of the radiation pattern. A six-element microstrip patch array designed using QCQP achieved 90° H-plane coverage with less than 1 dB gain variation [43], as illustrated in Fig. 1(b). The prototype maintained $\eta_{\text{RF-DC}}$ of around 50% across a wide set of arrival angles, validating QCQP for compact implementations. Key to this design was the use of reduced inter-element spacing with explicit modelling of mutual coupling, which ensured angular stability in a small footprint.

Large-scale flat-beam designs employ sequential feeding to improve robustness. A 196-element sequentially fed phased array demonstrated flat-top beam formation with axial ratio below 3 dB across the receiving plane, achieving 40% beam efficiency in drone WPT scenarios [44], as shown in Fig. 2(a). Sequential feeding also simplifies the network compared to corporate-fed designs while retaining adequate pattern control.Structural modifications offer an alternative approach. The compact aperture-coupled patch antenna shown in Fig. 2(b) integrates a mushroom structure to achieve flat-top circular polarization with 80° 3-dB beamwidths in both the E- and H-planes [45]. The design attains a peak gain of 8.5 dBi and maintains stable power reception under lateral displacements up to 60 mm, indicating tolerance to both angular and positional variations.

C. PERFORMANCE CHARACTERISTICS AND CRITICAL ANALYSIS

The performance of flat-beam rectennas can be categorized into two operational modes, as summarized in Table 3, with a consistent trade-off observed between angular coverage and peak rectifier efficiency $\eta_{\text{RF-DC}}$. Designs optimized for wider angular tolerance exhibit reduced peak efficiency, while configurations targeting higher $\eta_{\text{RF-DC}}$ achieve narrower coverage. For example, the QCQP-optimized six-element array reported in [43] maintains 50% $\eta_{\text{RF-DC}}$ over a 90° angular range. A larger-scale system employing a 32-element transmitter and a 37-element rectenna array achieves simulated efficiencies up to 80%, with measured values between 65.4% and 68.5%, while preserving angular stability [42]. Compact implementations emphasize coverage, with a flat-panel rectenna demonstrating a 144.6° half-power beamwidth and an $\eta_{\text{RF-DC}}$ of 51.8% [47]. Although these results confirm strong angular tolerance, most measurements are obtained under controlled laboratory settings with fixed loads and ideal matching. Their behaviour under realistic fluctuations in impedance, orientation, and incident field strength remains untested. Load optimisation also plays a crucial role in system-level performance. For an array of N identical rectifiers, the optimum load resistance scales as R_L/N for parallel connections and NR_L for series connections [42]. Proper application of this scaling is required to maximize power transfer and ensure stable DC output in practical deployments.

D. LIMITATIONS AND RESEARCH GAPS

Despite their advantages in mitigating angular misalignment, flat-beam rectennas face various limitations that remain open research challenges. A key gap in the literature is the lack of comprehensive demonstrations showing flat-beam rectennas powering functional electronic systems under realistic operating conditions. Although many studies report high $\eta_{\text{RF-DC}}$ and wide angular coverage, only a small fraction validate these designs by driving IoT sensors, wireless communication modules, or practical electronic loads in real-world environments. This disconnect between laboratory-focused characterization and system-level demonstrations remains a barrier to the broader adoption of flat-beam energy harvesters [48].

Flat-beam characteristics are optimized for narrow frequency bands and degrade when operated outside that range. Achieving flat-beam performance across wide or multi-band spectral regions remains challenging due to the frequency sensitivity of array excitation profiles and matching networks [49], [50]. This limitation is restrictive for ambient RF harvesting, which benefits from capturing energy across multiple communication bands. Although recent advances in broadband rectenna design show promising directions, integrating broadband or multiband operation with stable flat-beam performance remains largely unexplored.

A fundamental trade-off in flat-beam design is the reduction in peak gain compared to directive arrays with similar aperture sizes. This trade-off enables wide angular coverage but limits the maximum achievable received power, posing challenges for long-range WPT [51], [52]. The relationships among angular coverage, gain reduction, effective aperture, and maximum operational range remain insufficiently analyzed, leaving limited guidance for system designers. Moreover, maintaining low sidelobes outside the intended angular sector is nontrivial. Many reported flat-beam arrays exhibit elevated sidelobe levels, which can reduce overall system efficiency and increase susceptibility to interference from unintended directions. This issue becomes increasingly critical in dense urban or indoor RF environments, where multiple high-power emitters may be present. Scalability also presents a significant challenge. As array sizes increase, mutual coupling, feeding-network losses, and manufacturing tolerances make it difficult to maintain stable flat-beam profiles. The 196-element sequential array [44] demonstrates progress toward large-scale implementations; however, achieving comparable performance with larger apertures or at higher frequencies (e.g., millimeter-wave bands) remains an open research problem. These scalability issues highlight the need for new design methodologies, optimization frameworks, and fabrication techniques that can support large flat-beam array architectures.

V. MULTIDIRECTIONAL RECTENNAS

Multidirectional rectennas address angular misalignment through spatial diversity, using multiple antenna elements oriented in different directions to achieve quasi-omnidirectional coverage. Unlike flat-beam designs that modify the radiation pattern of a single aperture, multidirectional systems distribute reception across physically separated elements and combine their outputs to provide stable power delivery regardless of incident angle. This section reviews the architectural topologies, implementation strategies, and performance characteristics of multidirectional rectenna systems, while critically evaluating their current limitations and research gaps.

A. ARCHITECTURAL TOPOLOGIES FOR POWER COMBINING

The effectiveness of multidirectional rectennas depends on how power from multiple antenna elements is combined. Three topologies have emerged, each with distinct advantages and limitations, as illustrated in Fig. 3. In RF-combining architectures, outputs from multiple antenna elements are merged at the RF stage before entering a single rectifier. This is achieved using hybrid couplers, Wilkinson dividers/combiners, or transmission-line networks. Although RF combining can be efficient when signals are coherent and properly phased, it suffers from several drawbacks. It is highly sensitive to phase differences between signals arriving from different directions, which can lead to destructive interference. The combining network also introduces insertion losses that degrade overall efficiency. Most critically for multidirectional systems, RF combining can create unintended directional patterns that undermine the desired angular diversity [63].

DC combining addresses the limitations of RF combining by employing independent rectifiers for each antenna element, with their DC outputs combined in series (for voltage summation) or parallel (for current summation) configurations [28]. This topology offers several advantages. It eliminates phase sensitivity issues, allows each rectifier to operate at its optimal impedance point, and provides spatial diversity. Series connections improve output voltage ($V_{\text{DC}} = \sum V_n$), advantageous for low-power applications requiring higher voltage for circuit startup. Parallel connections increase current capability ($I_{\text{DC}} = \sum I_n$), beneficial for applications requiring higher power delivery. However, DC combining requires multiple rectifier circuits, increasing component count, cost, and potential for mismatch between individual rectifiers.

Hybrid combining represents a compromise approach that balances the advantages of both previous topologies [29]. In this architecture, antenna elements are grouped into subsets, and each subset undergoes RF combining before rectification. The resulting DC outputs from all rectifiers are then combined. This hierarchical method reduces the number of rectifiers compared with pure DC combining while maintaining better angular coverage than pure RF combining, since each subset still provides spatial diversity. The hybrid approach is particularly effective when a moderate number of elements, for example four to eight per subset, can provide adequate angular coverage within each subset.

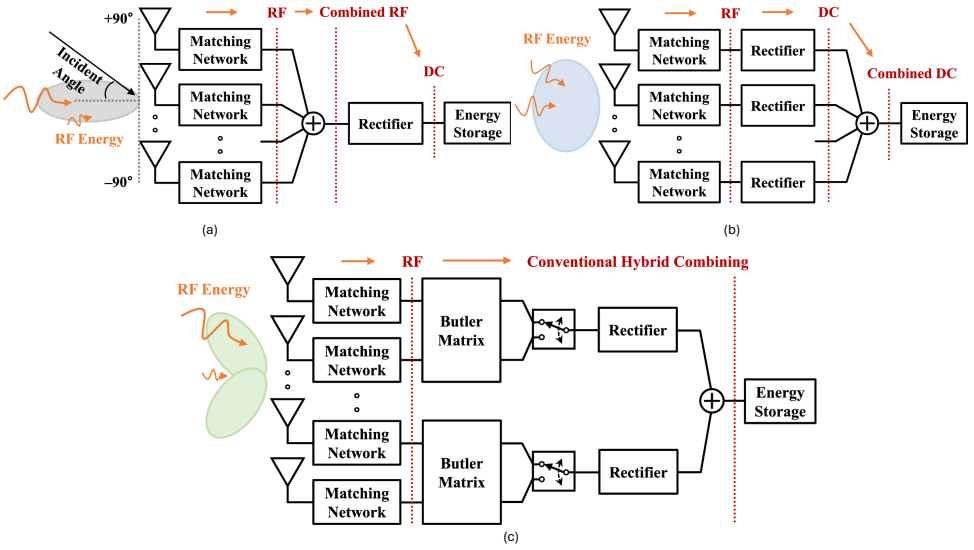

FIGURE 3. **Power combining topologies for multidirectional rectennas: (a) RF combining, where multiple antenna outputs are combined prior to rectification; (b) DC combining, where rectified outputs are combined at the DC stage; and (c) hybrid RF–DC combining, which integrates both approaches [29].**

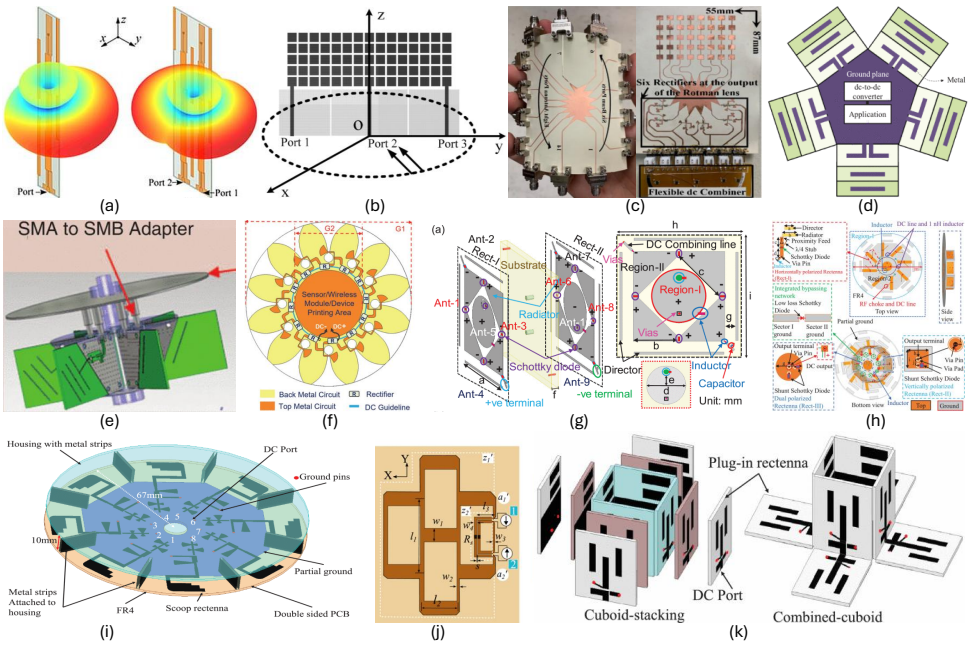

FIGURE 4. **Representative multidirectional rectenna designs: (a) Compact quasi-Yagi array [53]; (b) Multiport pixel rectenna [54]; (c) Rotman lens-based array [55]; (d) Quasi-Yagi multisector array [56]; (e) Six Yagi-Uda arrangement [57]; (f) Twelve Vivaldi radiators [58]; (g) Mirror-based design [32]; (h) Polarization-insensitive array [59]; (i) Dual-purpose radial rectenna [60]; (j) Grid-array rectenna [61]; (k) Plug-in multidirectional rectenna [62].**

B. DESIGN EVOLUTION AND IMPLEMENTATION STRATEGIES

Various multiport rectenna designs have been reported between 2016 to 2025 [7], [28], [30]–[32], [53], [54], [57]–[62], [66]–[84]. Fig. 4 presents representative multidirectional rectenna architectures, including compact implementations, advanced combining strategies, and lens-assisted designs. For space-limited applications, compact structures such as the quasi-Yagi array [53] and the plug-in multidirectional rectenna [62] achieve practical angular coverage with minimal footprint, making them suitable for small-form-factor devices. The grid-array rectenna [61] and the multiport pixel design [54] demonstrate advanced power-combining strategies. The grid-array employs a traveling-wave architecture with isolated ports to generate tilted dual beams, enabling wide-angle harvesting without complex beamforming networks. The pixel rectenna uses system-by-optimization (SEBO) methods to optimize multiport antenna behavior, showing the potential of computational synthesis for multidirectional operation. Although, multidirectional systems incorporate lens elements. The Rotman-lens-based array [55] achieves 140° coverage through a beamforming network, at

TABLE 4. Performance Comparison with State-of-the-Art Designs

Parameter/Ref./Year	[56]/2018	[57]/2016	[64]/2019	[30]/2023	[31]/2023	[65]/2023	[66]/2024	[32]/2025
Frequency (GHz)	2.45	2.45	2.45	5.8	5.2	$3.4-3.6$	5.8	5.2
Beams	5	6	20	12	9	Quasi	8	10
Sectors	5	6	5	6	8	2	8	10
SIBN[1]	No	No	No	NR[2]	NR	No	No	NR
Size (mm^3)	$250\times250\times0.8$	$160\times160\times60$	$130\times130\times290$	$130\times130\times1.56$	$74\times74\times1.56$	$50.3\times50.3\times11.5$	$60\times60\times11.12$	$25\times25\times1.56$
Beam Mechanism	Simple	Simple	Butler Matrix	Simple	Simple	Simple	Complex	Simple
Matching Network	Yes	Yes	Yes	CM[3]	CM	Yes	CM	CM
Gain (dBi)	10	2-7	~ 8	6.4	5	2	3.12	3.5
Isotropic DC Pattern	No	No	No	No	No	Quasi	Yes	Yes
Open DC Voltage (mV)	~ 400 at -12.5 dBm	~ 1800 at 0 dBm	~ 1400 at -10 dBm	~ 600 at -10 dBm	~ 600 at -10 dBm	1500 at 7 dBm	1103 at -10 dBm	~ 1600 at -10 dBm
Fabrication Complexity	Complex	Complex	Complex	Simple	Simple	Complex	Complex	Simple
Load (KΩ)	1 to 20	1$M\Omega$	5.1	1.28	1.2	2	2.8	2.48
$\eta_{\text{RF-DC}}$ (%)	~ 20	NG[4] Only DC voltage	45 NG NG	69.1 (EFR) 65.28 (BSR) NG	49 (EFR) 47 (BSR) NG	76.6 at 14 dBm	45.54	60.5 (Ant-1 and Ant-6) 55 (SDRS at $\theta=90^\circ$) 44.76 (SDRS at $\phi=0^\circ$)

[1]SIBN: Smart Integrated Bypass Network; [2]NR: Not reported; [3]CM: Conjugate matching; [4]NG: Not given.

the cost of increased footprint and complexity. This configuration represents an intermediate approach between fully multidirectional and lens-assisted architectures.

Some multidirectional rectennas targeted full azimuth coverage of 360°. A five sector planar quasi Yagi array achieved 20% efficiency at $2.45,\text{GHz}$ [56]. These designs, however, offered limited elevation coverage and reduced efficiency due to the trade off between sector count and aperture efficiency. A six and twelve element design provides three-dimensional coverage [57], [58], although analytical discussion of their performance remains limited. Subsequent implementations employed beamforming networks to enhance coverage. A design incorporating a miniaturized twenty port Butler matrix achieved 97% spherical coverage, corresponding to 3.87π sr, with 38% efficiency under low ambient power conditions [64]. Beamforming networks, however, introduce added complexity, larger physical volume, and insertion loss, reducing their suitability for compact IoT or batteryless sensor applications.

Recent work has emphasized achieving three dimensional coverage with simplified architectures. A key development is the integration of end fire and boresight elements within each sector. An eight element planar array containing one boresight element and multiple end fire elements achieved uniform DC harvesting across azimuth and elevation using conjugate matching and DC combining, reaching $\eta_{\text{RF-DC}}$ values up to 69.1% [30], [31]. This method avoids complex beamforming networks while preserving broad coverage. A two layer PCB using mirror symmetric end fire and boresight rectifying antennas achieved quasi isotropic three dimensional coverage with 60.5% efficiency through full wave rectification [32]. Polarization insensitive designs that combine horizontally and vertically polarized elements with a central cross polarized patch produced near isotropic patterns with 58.9% efficiency, mitigating polarization related misalignment [59]. To improve elevation coverage without increasing the complexity of individual arrays, stacked configurations have been investigated. Two planar multisector rectenna arrays arranged with a 45° offset enhanced both elevation and azimuth coverage [66]. This approach exploits modularity while addressing the difficulty of achieving comprehensive spherical coverage using predominantly planar structures.

C. PERFORMANCE ANALYSIS AND COMPARISON

Table 4 presents a comparison of recent multi-beam rectenna systems with wide angular coverage, focusing on operating frequency, beam configuration, physical size, and $\eta_{\text{RF-DC}}$. The reported peak $\eta_{\text{RF-DC}}$ range from 20% to 76.6%, with higher efficiencies achieved at moderate input power levels between -12.5 dBm to 7 dBm [30]–[32], [64], [65]. Rectennas employing conjugate matching networks consistently demonstrate higher conversion efficiency than designs using conventional matching networks.

The comparison reveals a trade-off between the number of beams and system complexity. Butler matrix-based architectures [64] support a high beam count with moderate antenna gain but require increased physical volume and fabrication complexity. In contrast, designs based on simple beamforming mechanisms [30]–[32] achieve comparable or higher $\eta_{\text{RF-DC}}$ with reduced size and lower antenna gain (2-6.4 dBi). Recent compact implementations further increase sector count while minimizing footprint; for instance, [32] integrates ten sectors within a $25\times25\ \text{mm}^2$ area and maintains efficiencies above 44%. Near-isotropic DC output characteristics [32], [66] enhance tolerance to variations in the angle of incidence. Most reported systems operate in the 2.45 GHz, 5.2/5.8 GHz, or sub-6 GHz bands, reflecting regulatory constraints and the availability of mature RF components.

D. CRITICAL ANALYSIS AND RESEARCH GAPS

Multidirectional rectenna literature reveals several open research gaps despite recent progress. A primary gap is absence of end-to-end demonstrations of multidirectional rectennas integrated into complete wireless power systems. Despite reports of high efficiency and wide angular coverage, existing designs have not been validated through full energy-harvesting cycles that include energy storage, power management, and practical load operation. This gap between component-level performance and system-level functionality continues to hinder real-world deployment. Most multidirectional designs operate in single or narrow frequency bands,

near 2.45 GHz or 5.8 GHz. This restricts effectiveness in ambient RF environments where available power spans multiple communication bands. Although recent work on broadband energy harvesting [49], [50] shows promising progress, combined realization of broadband operation with multidirectional coverage remains unaddressed. This challenge is reinforced by dependance on resonant structures for wide angular coverage, which inherently limits bandwidth.

The trade-offs among angular coverage, power conversion efficiency, and system complexity are not yet well characterized. Empirical results show that increasing sector count improves coverage but increase bulkiness and reduces efficiency because each sector introduces additional DC combining losses. Quantitative models for selecting appropriate sector count for specific applications remain limited. Recent analytical studies [7], [79] begin to address this problem, but more complete frameworks are needed that incorporate practical constraints such as impedance matching, combining losses, and realistic antenna behavior. Another limitation is common assumption of linear polarization and continuous wave excitation in multidirectional rectenna evaluations. Actual RF environments contain arbitrary polarization states and various modulation formats, and their impact on multidirectional architectures is not well quantified. Although some polarization diverse implementations have been investigated [59], achieving consistent performance under polarization and waveform variability remains an open research problem.

As sector counts increase to improve directional coverage, manufacturing tolerances and reliability become more critical. Small variations in element placement, orientation, or electrical properties can significantly degrade performance. Larger component counts also raise concerns related to cost, reliability, and production yield, issues rarely addressed in studies centered on proof of concept prototypes. Existing multidirectional rectennas are largely static, relying on fixed sector configurations and combining networks. In environments where signal direction, power level, and frequency vary over time, adaptive or reconfigurable architectures could provide substantial performance gains. Integration of sensing, control, and reconfiguration mechanisms remains an underexplored direction for future research.

VI. METASURFACE-ASSISTED LENS RECTENNAS

Metasurface assisted lens rectennas use engineered electromagnetic structures to address angular misalignment, frequency selectivity, and aperture efficiency challenges in WPT [89]. Gradient index lenses [90]–[92], artificial dielectric materials [93], and metasurfaces focus or steer incident energy [94] from multiple directions toward rectifying elements. This section reviews the design principles, implementation methods, and performance characteristics of lens based rectennas and relates their operation to earlier flat beam and multidirectional architectures.

A. FUNDAMENTAL PRINCIPLES AND DESIGN PHILOSOPHY

The operating principle of metasurface assisted lens rectennas is the transformation of an incident plane wave from a given direction into a localized focal region where rectifying elements are placed. Unlike conventional antennas based on geometric optics or phased arrays requiring active control, lens based systems perform beam shaping through material properties and structural configuration, enabling passive beam steering, improved aperture utilization, and frequency selective response [85]. Lens based systems provide direction dependent focusing without active components. An ideal Luneburg lens exhibits a refractive index profile given by

$$n(r) = \sqrt{2 - \left(\frac{r}{R}\right)^2}, \tag{1}$$

where R is the lens radius and r is the radial distance from the lens center. This index distribution causes plane waves incident from any direction to focus onto a point on the opposite surface, enabling multibeam reception with rectifiers positioned at the corresponding focal locations. Lens based rectennas concentrate incident energy collected over a large aperture onto compact rectifying elements and can achieve higher aperture efficiency than conventional array architectures. This property is relevant at millimeter wave frequencies, where rectifier impedance matching becomes difficult under low input power conditions [97], [98]. Metasurface and artificial dielectric implementations also enable frequency selective operation through structural resonance. This capability allows rectenna designs optimized for specific frequency bands while improving rejection of out of band signals, which is beneficial for RFEH in spectrally congested environments [99].

B. IMPLEMENTATION ARCHITECTURES AND TECHNOLOGIES

Fig. 5 illustrates the diversity of implementation approaches in metasurface-assisted lens rectennas, ranging from traditional dielectric lenses to advanced metasurface designs. Traditional dielectric lenses form the foundation of many lens-based rectenna systems. A lightweight dielectric Luneburg lens fabricated using 3D-printed metasurfaces demonstrated efficient multi-beam operation at 24 GHz, achieving 76% $\eta_{\text{RF-DC}}$ at 14.9 dBm input power [87]. This design connected 21 detector ports to a common load, enabling energy harvesting from two quadrants of angular space with uniform gain distribution. Additive manufacturing enabled complex gradient-index structures that would be difficult to realize through conventional fabrication. Metallic implementations provide an alternative means of achieving gradient-index behavior. A metallic Luneburg lens with 19 detector ports achieved 72% $\eta_{\text{RF-DC}}$ at 15.8 dBm input power at 26.5 GHz [95]. These designs often employ glide-symmetric or corrugated structures to emulate the required refractive-index profiles. Although potentially more lossy than dielectric implementations, metallic lenses offer advantages in mechanical robustness and thermal management.

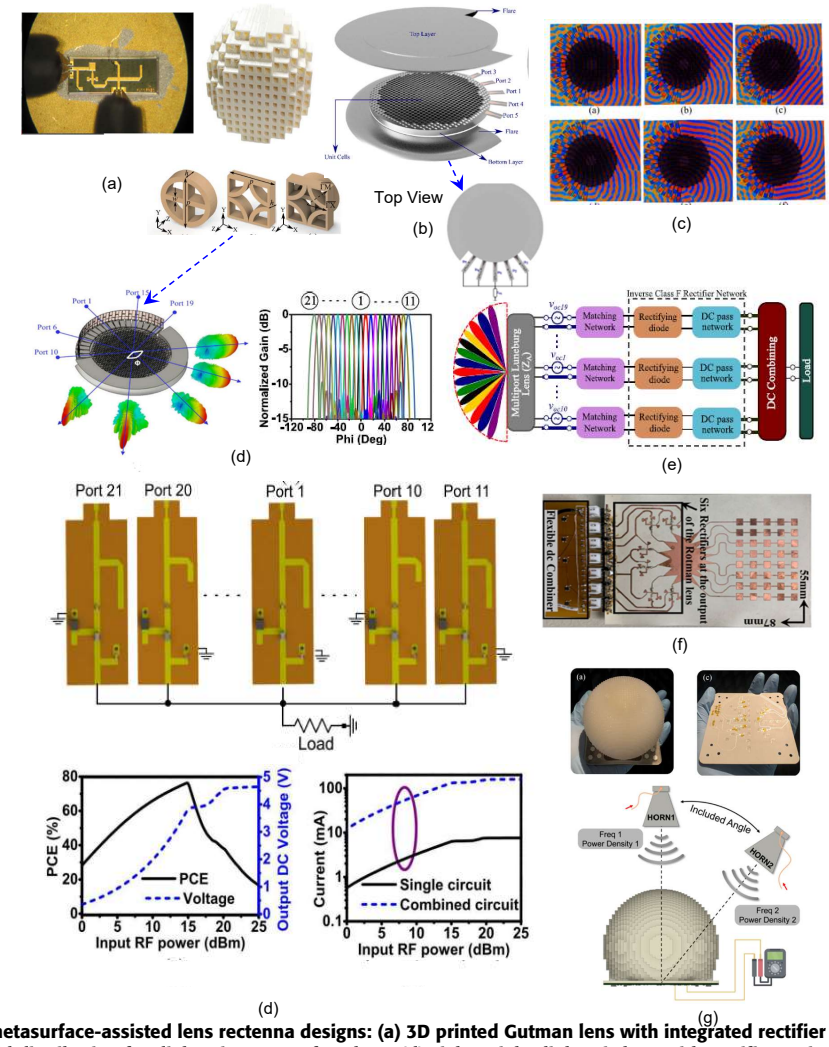

FIGURE 5. Representative metasurface-assisted lens rectenna designs: (a) 3D printed Gutman lens with integrated rectifier [85]; (b) Multi-port metallic Luneburg lens [86]; (c) E-field distribution for dielectric metasurface lens; (d) Lightweight dielectric lens with rectifier co-integration [87]; (e) System block diagram; (f) Flexible Rotman lens rectenna [55]; (g) Modified Luneburg lens prototype [88].

More advanced architectures integrate multiple focusing capabilities within a single structure. A 3D-printed Gutman lens demonstrated multi-focusing operation with 48% power-conversion efficiency at 210 mW input power [85]. Unlike Luneburg lenses, which focus incident waves onto the opposite surface, Gutman lenses can be designed to focus waves from specific directions to predetermined focal points, offering flexibility for targeted applications. For scenarios requiring mechanical flexibility or conformal mounting, polymer-based implementations have been explored. A flexible Rotman lens rectenna fabricated on a polyimide substrate demonstrated 110° angular coverage with a turn-on sensitivity of -6 dBm/cm^2 at 28 GHz [55]. The design maintained performance under bending, highlighting its potential for integration into wearable devices or curved surfaces [100].

C. PERFORMANCE ANALYSIS AND COMPARISON

Table 5 provides a comparison of metasurface-assisted lens rectenna designs, highlighting trends in performance and implementation complexity, including efficiency characteristics, angular coverage, beam behavior, frequency response, and bandwidth. Lens-based rectennas exhibit peak efficiencies in the range of 40-76%, with higher values corresponding to input power levels of 10-23 dBm [55], [85]–[88], [95], [96]. This efficiency range is competitive with other architectures, though direct comparison is complicated by differing measurement conditions and system configurations. Efficiency also varies significantly with angle of incidence, with peak performance occurring at design-specified focal directions.

The angular coverage of lens-based systems is discrete rather than continuous, as efficient energy harvesting occurs only from directions aligned with rectifier placement at focal points. Systems such as the 58-port modified Luneburg lens [88] achieve wide coverage (130° 3D coverage) through dense focal-point distribution, albeit with increased structural complexity and physical size. Most reported designs operate at specific millimeter-wave frequencies (24-40 GHz), leveraging regulatory allowances for higher EIRP and the reduced physical dimensions achievable at these frequencies. The modified Luneburg lens [88] demonstrates exceptional bandwidth (24-40 GHz, 50% relative bandwidth), though this

TABLE 5. Performance Comparison of the Metasurface Assisted Antennas

Ref/Year	Radiator	No. of ports	Freq (GHz)	Max Gain (dBi)	Rectifier topology, Diode	Max PCE ($\eta_{\text{RF-DC}}$) (%)	Remarks
[55]/2021	Flexible Rotman lens	14	28	17	Single Series MA4E2038	Turn-on: -6 dBm/cm^2	Planar, flexible, wide coverage, bending-resilient
[86]/2021	2D GRIN Luneburg lens	5	24	17.2	Single Series MA4E1317	63 @ 9.5 dBm	Planar, bulky narrow coverage
[95]/2022	Metallic Luneburg lens	19	26.5	18	Class F MA4E1317	72 @ 15.8 dBm	Planar, bulky narrow coverage
[87]/2022	Dielectric Luneburg lens	21	24	19.6	Inverse Class F MA4E1317	76 @ 14.9 dBm	Planar, Light weight narrow coverage
[96]/2023	Metallic Luneburg lens	3	25	17.3	Single Series MA4E1317	62 @ 12.5 dBm	Planar, compact narrow coverage
[85]/2024	3D printed Gutman lens	1	24	NA	Class F Load MMIC	48 @ 23 dBm	Non-Planar, multi--focusing, On-chip rectification
[88]/2024	3D printed Modified Luneburg Lens	58	24-40	27	Single Series SDM02U30LP3-7B	40-60 % @ -6 dBm per unit area per transmitter	Non-Planar, wide--coverage, High gain dual-linear

is uncommon; most lens-based architectures remain relatively narrowband due to their resonant or quasi-optical nature.

D. CRITICAL ANALYSIS AND RESEARCH GAPS

Despite their promising characteristics, metasurface-assisted lens rectennas face several persistent challenges, including fabrication complexity and cost, size and weight constraints, integration with rectification circuits, thermal management, limited real-world validation, and discrepancies between theoretical predictions and experimental results [101]. The fabrication of gradient-index lenses, especially those requiring precise three-dimensional structures or intricate metasurface patterns remains a major obstacle. Although additive manufacturing offers a path toward complex geometries, current techniques often lack the resolution or material consistency needed for optimal millimeter-wave performance. Moreover, cost, scalability, and yield considerations for mass production are seldom addressed in the literature, despite being critical for practical deployment.

While lens-based systems can be compact at millimeter-wave frequencies, their physical dimensions scale with wavelength [102]. At lower frequencies (e.g., sub-6 GHz ambient RF bands), practical lens apertures become prohibitively large for many IoT applications. This frequency–size dependency restricts lens-based approaches to higher-frequency scenarios or specialized use cases where physical size is less constrained. Integration with rectification circuits presents additional challenges. The physical separation between the lens aperture and rectifying elements requires feed networks that introduce insertion loss and design complexity, particularly as the number of focal ports increases. Some designs attempt direct integration of rectifiers at focal points, but this approach complicates thermal management and limits flexibility in rectifier topology and matching network design.

The concentration of RF energy at focal points results in localized power densities that can exacerbate thermal issues, especially under higher input power levels. Designs embedding rectifiers at focal locations face thermal stress, which can impair long-term reliability. Despite its importance, thermal analysis is often treated superficially or omitted altogether in existing studies [103], [104]. A further limitation is the scarcity of demonstrations in realistic operating environments. Most reported results rely on controlled laboratory setups with stable illumination, ideal impedance matching, and fixed incidence conditions. The performance of lens-assisted rectennas under practical variations, such as fluctuating angles of arrival, polarization mismatch, and interference, is largely unexplored. Additionally, several advanced designs, particularly those incorporating complex metasurface structures, have been validated primarily through simulations rather than physical prototyping [87]. The transition from simulation to hardware often reveals deviations stemming from material dispersion, fabrication tolerances, or parasitic coupling, which can significantly reduce real-world performance.

E. MILLIMETER-WAVE IMPLEMENTATION CONSIDERATIONS

The majority of advanced lens-based rectenna designs operate at millimeter-wave frequencies (24-40 GHz), which presents both opportunities and challenges. At 24 GHz, regulatory bodies such as the Federal Communications Commission (FCC) permit effective isotropic radiated power (EIRP) levels up to 75 dBm for point-to-multipoint systems [55]. With practical antenna gains of 25 dBi for both transmitter and receiver, this restricts transmitter power to 21 dBm (0.125 W) [40]. Given these limitations, achieving received power levels of 10-15 dBm requires transmission distances less than 1 meter according to the Friis transmission equation. Within these limited ranges, lens-based rectennas find potential applications in several domains, such as,

- **5G IoT Device Powering:** Short-range wireless charging of sensors and devices in office or factory environments within 0.5-1 meter range.
- **Wearable Electronics:** Wireless power delivery to body-worn devices where close proximity to power sources is feasible.

TABLE 6. Unified Comparative Analysis of Angularly Robust Rectenna Architectures

Evaluation Dimension	Flat-Beam Rectennas	Multidirectional Rectennas	Metasurface-Assisted Lens Rectennas
Fundamental Principle	Engineered uniform gain profile over angular sector	Spatial diversity through multiple discrete elements	Passive wavefront shaping via gradient-index materials
Angular Coverage Type	Continuous wide sector	Quasi-omnidirectional (continuous or discrete)	Multiple discrete beams
Typical Angular Coverage	70-150° half-power beamwidth	360° azimuthal, ±60° elevation	Discrete directions (e.g., 5-21 beams)
Peak $\eta_{\text{RF-DC}}$ Range	50-80%	20-70%	40-76%
Optimal Frequency Range	Sub-6 GHz (for practical sizes)	Sub-6 GHz	Millimeter-wave (24-40 GHz)
Implementation Complexity	Moderate (array optimization)	Low to High (depends on element count)	High (lens fabrication, integration)
Fabrication Challenges	Precise excitation control	Inter-element isolation, combining networks	Gradient-index realization, alignment tolerances
Physical Size Consideration	Moderate (scales with wavelength)	Compact to Moderate	Large at low frequencies, compact at mmWave
Power Consumption	None (passive)	None (passive combining)	None (passive)
Adaptability to Environment	Fixed pattern	Fixed or limited reconfiguration	Typically fixed, some tunable variants
System Integration Challenges	Load matching for array configurations	Multiple rectifier synchronization	Lens-rectifier interface, thermal management
Technology Readiness Level	Medium (laboratory prototypes)	Medium to High (some commercial products)	Low to Medium (mostly research prototypes)
Cost Considerations	Moderate (array fabrication)	Low to Moderate (multiple simple elements)	High (precision lens/metasurface fabrication)
Scalability Limitations	Pattern distortion with large arrays	Element count vs. coverage trade-off	Lens size vs. beam count trade-off

- **Industrial Automation:** Powering sensors on machinery or robotic systems where devices operate in predictable locations relative to power transmitters.
- **Laboratory-Scale Demonstrations:** Research platforms for WPT concepts, including potential applications in space-based solar power transmission [55].

The modified Luneburg lens design with 58 ports [88] represents perhaps the most technologically advanced implementation, featuring 27 dBi gain across 24-40 GHz bandwidth and delivering 3.5 V DC output at 0.15 mW/cm^2 power density. This design incorporates a serial power summation rectifier network to combine harvested power from multiple ports, addressing the integration challenge mentioned earlier. However, even this advanced design has not been demonstrated in a complete wireless power system powering functional loads.

VII. COMPARATIVE ANALYSIS AND FUTURE DIRECTIONS

The preceding sections have examined three distinct architectural paradigms for achieving angularly robust WPT flat-beam rectennas, multidirectional rectennas, and metasurface-assisted lens rectennas. Each approach addresses the fundamental challenge of angular misalignment through different physical principles, with corresponding trade-offs in performance, complexity, and implementation feasibility. This section provides a unified comparative analysis of these architectures, identifies critical research gaps across all three approaches, and outlines promising future directions for the field. To facilitate architectural selection based on application requirements, Table 6 presents a comprehensive comparison of the three paradigms across multiple dimensions. This framework extends beyond simple performance metrics to include practical implementation considerations that are crucial for real-world deployment.

A. CRITICAL ANALYSIS OF CURRENT LIMITATIONS

1) Lack of Comprehensive System Demonstrations

A major gap across existing rectenna architectures is the limited demonstration of complete wireless power systems operating under realistic conditions. Most reported works focus on component-level characterization, evaluating $\eta_{\text{RF-DC}}$ using fixed loads, controlled impedance matching, and stable continuous-wave excitation. While these measurements are useful for benchmarking rectifier performance, they do not capture system-level behavior when integrated with power management circuits, energy storage elements, and practical loads. Furthermore, experimental validation is generally confined to laboratory environments, with small consideration given to multipath propagation, time-varying incident power [105], temperature effects [106], or electromagnetic interference experienced in real-world deployments. Long-term operation and reliability under continuous or intermittent excitation are also rarely reported [32]. As a result, the impact of load variability, energy buffering, and control overhead on sustained system performance remains insufficiently characterized, limiting assessment of practical feasibility for real-world wireless power harvesting applications.

2) Frequency Limitations and Theory-Experiment Gaps

Most flat-beam, multidirectional, and lens-based rectenna designs operate in narrow frequency bands, centered at 2.45 GHz or 5.8 GHz [30]–[32], [58], [64], [65], while lens-based systems often target higher frequencies in the 24-40 GHz range [85]–[88], [95], [96]. Such narrowband operation limits their effectiveness for RFEH, where available power is distributed across multiple communication bands. Achieving wide angular coverage relies on resonant structures, which further constrains bandwidth and introduces a trade-off between frequency coverage and angular response.

Despite its importance, this trade-off remains insufficiently explored in existing studies.

In addition, a persistent gap exists between theoretical predictions and experimental performance, particularly for electrically large or structurally complex architectures. Several metasurface-assisted and lens-based rectenna concepts have been validated only through numerical simulations [87], while practical implementations often reveal fabrication tolerances, material losses, and integration challenges that degrade performance. Even for experimentally demonstrated flat-beam and multidirectional rectennas, measured $\eta_{\text{RF-DC}}$ frequently fall below simulated values, suggesting the presence of unmodeled losses in feeding networks, matching circuits, and rectifying devices [32], [53]–[62]. This gap indicates the need for experimentally validated designs and modeling approaches that account for non-ideal effects in practical implementations.

3) Scalability and Manufacturing Constraints

Scalability remains a limitation across flat-beam, multidirectional, and lens-based rectenna architectures, driven by different physical and practical constraints [62]. In flat-beam rectenna arrays, preserving uniform gain over wide angles becomes increasingly challenging as array size increases, due to strong mutual coupling, phase errors, and the rising complexity of power distribution and feeding networks [44]. For multidirectional rectennas, increasing angular coverage through additional radiating or rectifying elements reduces aperture utilization per sector, increases insertion losses, and adds integration overhead, which together limit system-level efficiency gains. Lens-based rectennas face an inherent size–frequency scaling constraint, as electrically large apertures are required to achieve directive or quasi-isotropic responses at lower frequencies, rendering sub-6 GHz implementations bulky and impractical for many applications [89]. Beyond electromagnetic performance, manufacturing considerations are rarely treated with sufficient rigor in existing studies. Issues such as fabrication tolerances, assembly repeatability, yield degradation with increased element count, and the cost implications of multilayer or three-dimensional structures are seldom quantified. The absence of tolerance-aware design and manufacturability analysis represents a significant barrier to scaling laboratory prototypes into deployable or commercially viable systems.

4) Lack of Standardized Benchmarking and Evaluation

Progress in multidirectional, flat-beam and metasurface lens rectenna research remains limited due to the absence of standardized benchmarking methodologies. Reported results vary widely in terms of incident power levels, polarization assumptions, load conditions, angular sampling resolution, and definitions of $\eta_{\text{RF-DC}}$, often without sufficient justification or normalization. As a result, direct comparison across different architectural approaches is unreliable, and reported performance improvements are difficult to contextualize. The lack of reference test scenarios or agreed-upon figures of merit hinders objective assessment of trade-offs among efficiency, angular coverage, bandwidth, and physical size. Establishing standardized evaluation frameworks and benchmark test cases would enable more meaningful cross-comparison, clarify performance limits, and guide architecture selection for application-specific wireless power harvesting scenarios.

5) Economic and Commercialization Viability

Beyond technical performance, the path to commercialization remains largely unexplored. A critical research gap is the comprehensive techno-economic analysis of angularly robust rectenna systems. Key unanswered questions include the cost-per-unit efficiency gains of complex architectures like lens-based systems; the energy return on investment (EROI) for manufacturing advanced metasurfaces; and the total cost of ownership when deployed in real-world IoT networks. Furthermore, business models for deploying such infrastructure, whether user-owned, service-provider-based, or public-utility models, are absent from the technical literature. Addressing these economic viability questions is essential for transitioning from laboratory prototypes to scalable, sustainable wireless power solutions.

B. CONVERGENT RESEARCH DIRECTIONS

1) Broadband and Multiband Operation

Enabling broadband or multiband operation while preserving angular robustness remains a largely unresolved challenge in multidirectional and flat-beam rectenna design. Most existing architectures rely on resonant elements and frequency-specific matching networks, which inherently limit usable bandwidth. Future progress therefore requires architectural innovations that decouple angular coverage from narrowband resonance behavior. Several research directions show potential in this context.

- Incorporation of tunable or reconfigurable components, such as varactors, RF switches, or adaptive matching networks, to enable dynamic operation across multiple frequency bands and to respond to variations in the spectral distribution of ambient RF energy [107]. However, the additional insertion loss, control overhead, and nonlinearity introduced by tuning elements must be carefully considered.
- Use of broadband or frequency-independent antenna elements combined with frequency-selective power combining or rectification stages, allowing different bands to be processed independently while sharing a common aperture.
- Application of dispersion engineering and multi-resonant unit cells to tailor angular and frequency responses simultaneously, although fabrication tolerances and loss mechanisms pose significant implementation challenges.

Recent studies on broadband RF energy harvesting [49], [50] provide useful insights into wideband rectification and matching strategies; however, their extension to architectures with robust multidirectional or flat-beam characteristics remains largely unexplored.

2) Adaptive and Intelligent Systems

The integration of adaptive and intelligent control mechanisms represents a promising direction for overcoming the limitations of static rectenna architectures in dynamic RF environments. Ambient wireless power conditions vary significantly with time, location, frequency occupancy, and user activity, motivating designs capable of real-time reconfiguration [108]–[115].

- Dynamic tuning of matching networks in response to changes in incident power level, frequency content, or load conditions to maintain near-optimal $\eta_{\text{RF-DC}}$.
- Selective activation or weighting of antenna elements, beams, or rectification paths based on incident signal direction and strength, improving effective aperture utilization and reducing unnecessary losses.
- Use of environmental sensing combined with machine learning or heuristic optimization algorithms to adjust system configuration under uncertain and time-varying conditions.

While such adaptive approaches offer the potential for substantial performance gains, they introduce additional circuit complexity, control latency, and power consumption. Careful system-level co-design is therefore required to ensure that the net harvested energy remains positive, particularly in low-power ambient harvesting scenarios.

3) Multi-Function Integration and Material-Fabrication Innovations

Future wireless power harvesting platforms are expected to evolve beyond standalone rectennas toward multi-function systems that share apertures, circuitry, and packaging with additional capabilities. One emerging direction is the integration of RF energy harvesting with sensing or localization functions, enabling dual-use hardware for applications such as distributed monitoring, asset tracking, and Internet-of-Things (IoT) nodes [116]–[120]. Such integration, however, introduces design trade-offs related to shared bandwidth, interference between sensing and harvesting modes, and competing requirements on antenna radiation characteristics [98]. Thermal considerations also become increasingly important as system integration density and input power levels increase. Co-design of electromagnetic and thermal management strategies is therefore necessary, for compact or high-power implementations, to ensure stable operation and prevent performance degradation of rectifying and control circuits [121]. Advances in materials and fabrication technologies can address key challenges related to scalability, bandwidth, and form factor in rectenna systems. Additive manufacturing enables complex three-dimensional and graded-index structures, while flexible electronics support conformal and wearable integration. Tunable and smart materials offer reconfigurability but introduce loss and control challenges. Low-cost, high-yield fabrication remains essential for large-scale and practical deployment.

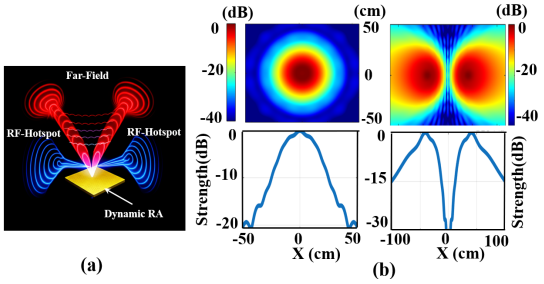

FIGURE 6. Concept of a dynamic metasurface antenna for location-aware wireless power transfer through adaptive field shaping.

C. EMERGING PARADIGMS AND FUTURE VISION

Several emerging paradigms address the key limitations identified earlier in this review, including narrowband operation, limited angular robustness under dynamic conditions, lack of system-level adaptability, and scalability constraints. Dynamic metasurface antennas (DMAs) represent a potential fourth architectural paradigm that targets the need for adaptive, system-level solutions. As illustrated in Fig. 6, DMAs employ tunable unit cells to dynamically shape the transmitted electromagnetic field, enabling location-aware RF energy hotspots that can track device motion and adapt to environmental changes. This capability mitigates the limitations of static beam patterns and reduces reliance on complex receiver-side architectures. Near-field focusing and wireless power surfaces address misalignment and coverage challenges inherent to flat-beam and multidirectional rectennas by shaping the spatial energy distribution in the near field. These approaches alleviate the trade-off between angular coverage and efficiency, enabling power delivery over extended regions without precise alignment or increased receiver complexity. Holographic and machine-learning-optimized designs target the theory-experiment performance gap by enabling inverse and data-driven synthesis of antenna and metasurface structures that incorporate fabrication tolerances, losses, and environmental variability, leading to improved agreement between simulated and measured performance. Quantum-inspired and non-radiative energy transfer concepts relate to the fundamental alignment and bandwidth limitations of resonant far-field architectures. These approaches rely on engineered near-field coupling instead of radiative propagation, providing a potential pathway to relax angular alignment constraints, although substantial theoretical and practical challenges persist.

D. APPLICATION-ORIENTED SELECTION GUIDE

The comparative evaluation of angularly robust rectenna architectures shows that architecture selection depends on the angular distribution of incident RF energy, device mobility, and system efficiency requirements. No single architecture is optimal across all deployment scenarios. Fig. 7 summarizes the correspondence between representative application conditions and suitable rectenna architectures. Multidirectional rectennas provide consistent performance in applications where both device orientation and incident signal direction vary unpredictably. Their reliance on spatial diversity

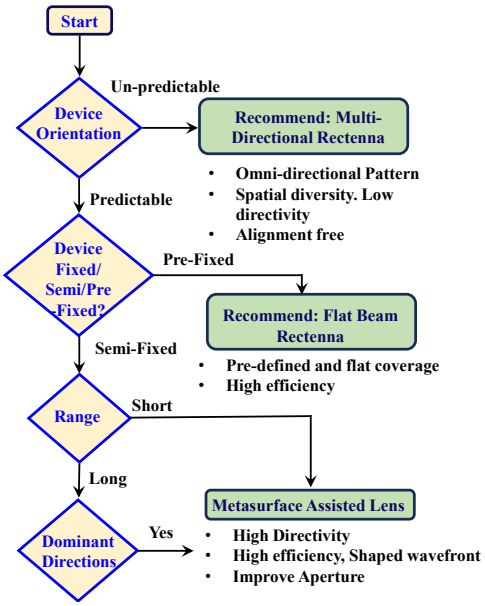

FIGURE 7. Selection Guide for Rectenna Architectures Based on Application Requirements

enables energy capture from multiple angles without alignment constraints, making them suitable for wearable devices, mobile nodes, and ambient RF energy harvesting scenarios.

Flat-beam rectennas are better suited to fixed or semi-fixed installations operating within known spatial regions. These designs maintain relatively uniform received power over predefined angular sectors while preserving higher RF–DC conversion efficiency than omnidirectional approaches, which is advantageous for sensors mounted on infrastructure, machinery, or charging surfaces. Metasurface-assisted lens rectennas address scenarios where incident RF energy arrives predominantly from known directions. Passive wavefront shaping increases effective aperture and received power without active beam control, making these architectures appropriate for short-range indoor deployments and controlled WPT environments, albeit with reduced flexibility and higher structural complexity. Overall, the selection guide clarifies how trade-offs among angular coverage, conversion efficiency, and implementation complexity influence rectenna architecture suitability for practical wireless power harvesting applications.

VIII. CONCLUSION

This review has systematically examined three principal architectural paradigms for achieving angularly robust wireless power transfer (WPT), flat-beam rectennas, multidirectional rectennas, and metasurface-assisted lens rectennas. Each approach addresses angular misalignment through distinct mechanisms and exhibits characteristic trade-offs among angular coverage, $\eta_{\text{RF-DC}}$, implementation complexity, operating frequency, and scalability. Flat-beam rectennas provide stable power delivery over predefined angular sectors and are well suited for fixed deployments with predictable orientations. Multidirectional rectennas exploit spatial diversity to achieve quasi-omnidirectional coverage, offering more robustness for mobile, wearable, and ambient energy harvesting applications, albeit with moderate efficiency and increased circuit complexity. Metasurface-assisted lens rectennas enable high-efficiency, direction-specific power transfer through passive wavefront shaping, making them attractive for point-to-multipoint or high-performance systems, at millimeter-wave frequencies. Despite substantial progress, several challenges remain common across all architectures. These include the lack of end-to-end system demonstrations under realistic operating conditions, predominantly narrowband operation that limits ambient RF harvesting, discrepancies between simulated and experimental performance, and unresolved issues related to manufacturing scalability and benchmarking standardization. Addressing these gaps is essential for transitioning from laboratory prototypes to deployable wireless power systems. Near-term research priorities should focus on complete system-level demonstrations, standardized evaluation methodologies, broadband and frequency-agile designs, and manufacturable architectures. Medium-term efforts are expected to emphasize adaptive and multifunctional systems that integrate sensing, control, and communication capabilities, as well as hybrid architectures that combine complementary strengths of existing paradigms. In the longer term, emerging concepts such as dynamic metasurface antennas, wireless power surfaces, and data-driven electromagnetic design methodologies may enable new approaches to angularly robust WPT. As these challenges are addressed, angularly robust WPT is expected to mature from proof-of-concept demonstrations into practical technology capable of supporting maintenance-free, cable-free operation for distributed IoT, sensing, and mobile electronic systems.

REFERENCES

[1] M. Collotta and G. Pau, "An innovative approach for forecasting of energy requirements to improve a smart home management system based on BLE," *IEEE Transactions on Green Communications and Networking*, vol. 1, no. 1, pp. 112–120, 2017.

[2] C. Yu, K. Kam, Y. Xu, Z. Cui, D. Steingart, M. Gorlatova, P. Culligan, and I. Kymissis, "Plant spike: A low-cost, low-power beacon for smart city soil health monitoring," *IEEE Internet of Things Journal*, vol. 7, no. 9, pp. 9080–9090, 2020.

[3] H. Zadgaonkar and M. Chandak, "Locating objects in warehouses using BLE beacons & machine learning," *IEEE Access*, vol. 9, pp. 153116–153125, 2021.

[4] L. Li, X. Zhang, C. Song, W. Zhang, T. Jia, and Y. Huang, "Compact dual-band, wide-angle, polarization-angle-independent rectifying metasurface for ambient energy harvesting and wireless power transfer," *IEEE Transactions on Microwave Theory and Techniques*, vol. 69, no. 3, pp. 1518–1528, 2021.

[5] Y.-H. Suh and K. Chang, "A high-efficiency dual-frequency rectenna for 2.45- and 5.8-GHz wireless power transmission," *IEEE Transactions on Microwave Theory and Techniques*, vol. 50, no. 7, pp. 1784–1789, 2002.

[6] C. Liu, H. Lin, Z. He, and Z. Chen, "Compact patch rectennas without impedance matching network for wireless power transmission," *IEEE Transactions on Microwave Theory and Techniques*, vol. 70, no. 5, pp. 2882–2890, 2022.

[7] M. Kumar, S. Kumar, and A. Sharma, "An analytical framework of multisector rectenna array design for angular misalignment tolerant RF power transfer systems," *IEEE Transactions on Microwave Theory and Techniques*, pp. 1–13, 2022.

[8] N. Shinohara, "Trends in wireless power transfer: WPT technology for energy harvesting, millimeter-wave/THz rectennas, MIMO-WPT, and advances in near-field WPT applications," *IEEE Microwave Magazine*, vol. 22, no. 1, pp. 46–59, 2021.

[9] C. Zhang, W. Lu, J. Zhao, X. Wu, H. Chen, and D. Xu, "A novel asymmetric magnetic coupler applied to multiple-receiver wireless charging system for automated guided vehicles," *IEEE Transactions on Power Electronics*, vol. 38, no. 11, pp. 14761–14775, 2023.

[10] S. Xie, L. Wu, X. Zhang, J. Huang, and L. Li, "Misalignment-tolerant wireless power transfer system based on double-layer quadrature double-d coil with magnetic field control," *IEEE Transactions on Transportation Electrification*, vol. 10, no. 4, pp. 9945–9958, 2024.

[11] X. Duan, W. Han, Y. Hu, H. Tian, and J. Huang, "2-D misalignment-tolerant wireless power transfer with a compact O-to-OXY magnetic coupler," *IEEE Journal of Emerging and Selected Topics in Industrial Electronics*, vol. 6, no. 1, pp. 9–18, 2025.

[12] R. Inoue, Y. Inoue, H. Ueda, and S. Kim, "Investigation of hts coil structure robustness against misalignment between coils in a wireless power transmission system for railway vehicles," *IEEE Transactions on Applied Superconductivity*, vol. 33, no. 5, pp. 1–5, 2023.

[13] N. A. Pantazis, S. A. Nikolidakis, and D. D. Vergados, "Energy-efficient routing protocols in wireless sensor networks: A survey," *IEEE Communications Surveys Tutorials*, vol. 15, no. 2, pp. 551–591, 2013.

[14] S. Hemour, Y. Zhao, C. H. P. Lorenz, D. Houssameddine, Y. Gui, C.-M. Hu, and K. Wu, "Towards low-power high-efficiency RF and microwave energy harvesting," *IEEE Transactions on Microwave Theory and Techniques*, vol. 62, no. 4, pp. 965–976, 2014.

[15] Z. Popovic, E. Falkenstein, and R. Zane, "Low-power density wireless powering for battery-less sensors," in *2013 IEEE Radio and Wireless Symposium*, pp. 31–33, 2013.

[16] D. Mishra, S. De, S. Jana, S. Basagni, K. Chowdhury, and W. Heinzelman, "Smart RF energy harvesting communications: challenges and opportunities," *IEEE Communications Magazine*, vol. 53, no. 4, pp. 70–78, 2015.

[17] W. A. Khan, R. Raad, F. Tubbal, P. I. Theoharis, and S. Iranmanesh, "RF energy harvesting using multidirectional rectennas: A review," *IEEE Sensors Journal*, vol. 24, no. 12, pp. 18762–18790, 2024.

[18] A. A. G. Amer, S. Z. Sapuan, N. Nasimuddin, A. Alphones, and N. B. Zinal, "A comprehensive review of metasurface structures suitable for RF energy harvesting," *IEEE Access*, 2023. Funded by Universiti Tun Hussein Onn Malaysia (UTHM) under TIER 1 research grant, H150.

[19] G. Moloudian, M. Hosseinifard, S. Kumar, R. B. V. B. Simorangkir, J. L. Buckley, C. Song, G. Fantoni, and B. O'Flynn, "RF energy harvesting techniques for battery-less wireless sensing, industry 4.0, and internet of things: A review," *IEEE Sensors Journal*, 2024. Volume PP, issue 99 — see DOI below.

[20] A. A. Eteng, H. H. Goh, S. K. A. Rahim, and A. Alomainy, "A review of metasurfaces for microwave energy transmission and harvesting in wireless powered networks," *IEEE Access*, vol. 9, pp. 27518–27539, 2021.

[21] M. Wagih, A. S. Weddell, and S. Beeby, "Millimeter-wave power harvesting: A review," *IEEE Open Journal of Antennas and Propagation*, vol. 1, pp. 560–578, 2020.

[22] Z. Wang, D. Lu, R. Li, and Y. Yu, "Flexible broadband rectifying array antenna based on printed liquid metal," *IEEE Transactions on Microwave Theory and Techniques*, vol. 73, no. 9, pp. 6001–6008, 2025.

[23] R. Chopra and G. Kumar, "Series-fed binomial microstrip arrays for extremely low sidelobe level," *IEEE Transactions on Antennas and Propagation*, vol. 67, no. 6, pp. 4275–4279, 2019.

[24] X. Cai, G. Wen, and Y.-X. Guo, "Shaped beam rectenna with enhanced coverage for indoor RF energy harvesting," in *2019 IEEE Asia-Pacific Microwave Conference (APMC)*, pp. 994–995, 2019.

[25] Q. Hao, S. Zheng, and K. Lu, "An siw horn antenna with flat-top beam for millimeter-wave applications," *IEEE Antennas and Wireless Propagation Letters*, vol. 23, no. 2, pp. 608–612, 2024.

[26] N. Shinohara, Y. Kagata, B. Yang, and T. Mitani, "Development of a high total efficiency beam-forming antenna with a flat-top beam in radiative-near-field wireless power transfer," in *2024 International Symposium on Antennas and Propagation (ISAP)*, pp. 1–2, 2024.

[27] Y. Luo, Z. Guo, N. Yan, W. An, and K. Ma, "A flat-top beam h-plane siw horn antenna based on beamforming," *IEEE Antennas and Wireless Propagation Letters*, vol. 23, no. 2, pp. 588–592, 2024.

[28] S.-T. Khang, D.-J. Lee, I.-J. Hwang, T.-D. Yeo, and J.-W. Yu, "Microwave power transfer with optimal number of rectenna arrays for midrange applications," *IEEE Antennas and Wireless Propagation Letters*, vol. 17, no. 1, pp. 155–159, 2018.

[29] S. Kim, H.-J. Dong, and H. L. Lee, "Hybrid power combining rectenna array for wide spatial coverage of self-powered iot devices," *IEEE Internet of Things Journal*, vol. 11, no. 22, pp. 37302–37311, 2024.

[30] M. Kumar, S. Kumar, A. S. Bhadauria, and A. Sharma, "A planar integrated rectenna array with 3-d-spherical dc coverage for orientation-tolerant wireless-power-transfer-enabled IoT sensor nodes," *IEEE Transactions on Antennas and Propagation*, vol. 71, no. 2, pp. 1285–1294, 2023.

[31] M. Kumar, S. Kumar, and A. Sharma, "A planar orbicular rectenna array system with 3-d uniform coverage for wireless powering of IoT nodes," *IEEE Transactions on Microwave Theory and Techniques*, vol. 71, no. 3, pp. 1366–1373, 2023.

[32] M. Kumar and A. Sharma, "A compact planar multisector rectenna array with full-wave rectification for 3D uniform wireless powering of iot nodes," *IEEE Transactions on Antennas and Propagation*, pp. 1–1, 2025.

[33] X. Gu, L. Grauwin, D. Dousset, S. Hemour, and K. Wu, "Dynamic ambient RF energy density measurements of montreal for battery-free iot sensor network planning," *IEEE Internet of Things Journal*, vol. 8, no. 17, pp. 13209–13221, 2021.

[34] H. Sun, Y.-x. Guo, M. He, and Z. Zhong, "A dual-band rectenna using broadband yagi antenna array for ambient RF power harvesting," *IEEE Antennas and Wireless Propagation Letters*, vol. 12, pp. 918–921, 2013.

[35] M. Piñuela, P. D. Mitcheson, and S. Lucyszyn, "Ambient RF energy harvesting in urban and semi-urban environments," *IEEE Transactions on Microwave Theory and Techniques*, vol. 61, no. 7, pp. 2715–2726, 2013.

[36] C. Song, P. Lu, and S. Shen, "Highly efficient omnidirectional integrated multiband wireless energy harvesters for compact sensor nodes of internet-of-things," *IEEE Transactions on Industrial Electronics*, vol. 68, no. 9, pp. 8128–8140, 2021.

[37] N. Shariati, W. S. T. Rowe, and K. Ghorbani, "RF field investigation and maximum available power analysis for enhanced RF energy scavenging," in *2012 42nd European Microwave Conference*, pp. 329–332, 2012.

[38] Z. Liang and J. Yuan, "Modelling and prediction of mobile service channel power density for RF energy harvesting," *IEEE Wireless Communications Letters*, vol. 9, no. 5, pp. 741–744, 2020.

[39] C. Zhang, Q. Cheng, J. Yang, J. Zhao, and T. J. Cui, "Broadband metamaterial for optical transparency and microwave absorption," *Applied Physics Letters*, vol. 110, no. 14, p. 143511, 2017.

[40] V. Camarchia, R. Quaglia, A. Piacibello, D. P. Nguyen, H. Wang, and A.-V. Pham, "A review of technologies and design techniques of millimeter-wave power amplifiers," *IEEE Transactions on Microwave Theory and Techniques*, vol. 68, no. 7, pp. 2957–2983, 2020.

[41] A. Ghazanfari, H. Tabassum, and E. Hossain, "Ambient RF energy harvesting in ultra-dense small cell networks: performance and trade-offs," *IEEE Wireless Communications*, vol. 23, no. 2, pp. 38–45, 2016.

[42] N. Takabayashi, N. Shinohara, T. Mitani, M. Furukawa, and T. Fujiwara, "Rectification improvement with flat-topped beams on 2.45-GHz rectenna arrays," *IEEE Transactions on Microwave Theory and Techniques*, vol. 68, no. 3, pp. 1151–1163, 2020.

[43] X. Cai, W. Geyi, and Y. Guo, "A compact rectenna with flat-top angular coverage for RF energy harvesting," *IEEE Antennas and Wireless Propagation Letters*, vol. 20, no. 7, pp. 1307–1311, 2021.

[44] N. Takabayashi, K. Kawai, M. Mase, N. Shinohara, and T. Mitani, "Large-scale sequentially-fed array antenna radiating flat-top beam for microwave power transmission to drones," *IEEE Journal of Microwaves*, vol. 2, no. 2, pp. 297–306, 2022.

[45] D. M. Nguyen, N. D. Au, and C. Seo, "Aperture-coupled patch antenna with flat-top beam for microwave power transmission," *IEEE Antennas and Wireless Propagation Letters*, vol. 21, no. 10, pp. 2130–2134, 2022.

[46] H. Sun and W. Geyi, "A new rectenna using beamwidth-enhanced antenna array for RF power harvesting applications," *IEEE Antennas and Wireless Propagation Letters*, vol. 16, pp. 1451–1454, 2017.

[47] Y. Han, E. Kim, and H. L. Lee, "Flat-panel-rectenna with broad RF energy harvesting coverage for wireless-powered sensor applications," *IEEE Access*, vol. 13, pp. 6146–6153, 2025.

[48] A. Alabsi, A. Hawbani, X. Wang, A. Al-Dubai, J. Hu, S. A. Aziz, S. Kumar, L. Zhao, A. V. Shvetsov, and S. H. Alsamhi, "Wireless power transfer technologies, applications, and future trends: A review," *IEEE Transactions on Sustainable Computing*, vol. 10, no. 1, pp. 1–17, 2025.

[49] S. Islam, M. Zada, U. R. Iman, and H. Yoo, "Multibeam circular endfire array incorporating highly efficient nona-band rectifiers for iot energy harvesting applications," *IEEE Internet of Things Journal*, vol. 11, no. 12, pp. 22768–22778, 2024.

[50] W. Wang, J. Zhang, X. Sun, H. Zu, and D. He, "A compact five-band omnidirectional RF ambient energy harvesting system for iot applications," *IEEE Access*, vol. 13, pp. 86110–86119, 2025.

[51] R. Eirey-Pérez, A. A. Salas-Sánchez, J. A. Rodríguez-González, and F. J. Ares-Pena, "Pencil beams and flat-topped beams with asymmetric sidelobes from circular arrays [antenna designer's notebook]," *IEEE Antennas and Propagation Magazine*, vol. 56, no. 6, pp. 153–161, 2014.

[52] J. Rodriguez, F. Ares, P. Lopez, and E. Moreno, "Quasi-analytical synthesis of moderate and large arrays radiating arbitrary "star-shaped" footprint patterns [antenna designer's notebook]," *IEEE Antennas and Propagation Magazine*, vol. 49, no. 5, pp. 105–112, 2007.

[53] Y.-Y. Hu, S. Sun, and H. Xu, "Compact collinear quasi-yagi antenna array for wireless energy harvesting," *IEEE Access*, vol. 8, pp. 35308–35317, 2020.

[54] S. Shen, C.-Y. Chiu, and R. D. Murch, "Multiport pixel rectenna for ambient RF energy harvesting," *IEEE Transactions on Antennas and Propagation*, vol. 66, no. 2, pp. 644–656, 2018.

[55] A. Eid, J. G. D. Hester, and M. M. Tentzeris, "5G as a wireless power grid," *Scientific Reports*, vol. 11, no. 1, p. 636, 2021.

[56] Y.-S. Chen and J.-W. You, "A scalable and multidirectional rectenna system for RF energy harvesting," *IEEE Transactions on Components, Packaging and Manufacturing Technology*, vol. 8, no. 12, pp. 2060–2072, 2018.

[57] F. Fezai, C. Menudier, M. Thevenot, T. Monediere, and N. Chevalier, "Multidirectional receiving system for RF to DC conversion signal: Application to home automation devices," *IEEE Antennas and Propagation Magazine*, vol. 58, no. 3, pp. 22–30, 2016.

[58] C. Song, P. Lu, and S. Shen, "Highly efficient omnidirectional integrated multiband wireless energy harvesters for compact sensor nodes of Internet-of-Things," *IEEE Transactions on Industrial Electronics*, vol. 68, no. 9, pp. 8128–8140, 2021.

[59] M. Kumar, S. Kumar, A. Sharma, V. K. Malav, and P. Rattanpal, "An orthogonally polarized multibeam rectenna system to imitate isotropic dc pattern for orientation-insensitive microwave power delivery," *IEEE Transactions on Components, Packaging and Manufacturing Technology*, vol. 14, no. 4, pp. 659–668, 2024.

[60] M. Kumar, S. Kumar, and A. Sharma, "Dual-purpose planar radial-array of rectenna sensors for orientation estimation and RF-energy harvesting at IoT nodes," *IEEE Microwave and Wireless Components Letters*, pp. 1–4, 2022.

[61] G. Reghunadhan and C. Saha, "A dual-port grid array rectenna for third-harmonic feedback enabled wireless power transfer systems," *IEEE Antennas and Wireless Propagation Letters*, vol. 24, no. 8, pp. 2612–2616, 2025.

[62] M. Kumar, S. Kumar, S. Jain, and A. Sharma, "A plug-in type integrated rectenna cell for scalable RF battery using wireless energy harvesting system," *IEEE Microwave and Wireless Technology Letters*, vol. 33, no. 1, pp. 98–101, 2023.

[63] S. Shen and B. Clerckx, "Beamforming optimization for mimo wireless power transfer with nonlinear energy harvesting: RF combining versus dc combining," *IEEE Transactions on Wireless Communications*, vol. 20, no. 1, pp. 199–213, 2021.

[64] E. Vandelle, D. H. N. Bui, T.-P. Vuong, G. Ardila, K. Wu, and S. Hemour, "Harvesting ambient RF energy efficiently with optimal angular coverage," *IEEE Transactions on Antennas and Propagation*, vol. 67, no. 3, pp. 1862–1873, 2019.

[65] L. Guo, H. Fang, X. Li, W. Yang, and K. Wu, "A rectenna design with quasi-full spatial coverage based on a compact dielectric resonator antenna," *IEEE Transactions on Antennas and Propagation*, vol. 71, no. 10, pp. 7870–7880, 2023.

[66] S. Kumar, M. Kumar, and A. Sharma, "A compact stacked multisector near-isotropic coverage rectenna array system for IoT applications," *IEEE Microwave and Wireless Technology Letters*, vol. 34, no. 1, pp. 123–126, 2024.

[67] S. Shen, C.-Y. Chiu, and R. D. Murch, "A dual-port triple-band l-probe microstrip patch rectenna for ambient RF energy harvesting," *IEEE Antennas and Wireless Propagation Letters*, vol. 16, pp. 3071–3074, 2017.

[68] M. Abdallah, J. Costantine, A. H. Ramadan, and Y. Tawk, "A rectenna system with power combining topology for improved power handling capabilities," *IEEE Sensors Letters*, vol. 2, no. 4, pp. 1–4, 2018.

[69] Y.-Y. Hu, S. Sun, H. Xu, and H. Sun, "Grid-array rectenna with wide angle coverage for effectively harvesting RF energy of low power density," *IEEE Transactions on Microwave Theory and Techniques*, vol. 67, no. 1, pp. 402–413, 2019.

[70] S. Shen, Y. Zhang, C.-Y. Chiu, and R. Murch, "An ambient RF energy harvesting system where the number of antenna ports is dependent on frequency," *IEEE Transactions on Microwave Theory and Techniques*, vol. 67, no. 9, pp. 3821–3832, 2019.

[71] H. S. Vu, N. Nguyen, N. Ha-Van, C. Seo, and M. Thuy Le, "Multiband ambient RF energy harvesting for autonomous IoT devices," *IEEE Microwave and Wireless Components Letters*, vol. 30, no. 12, pp. 1189–1192, 2020.

[72] Y.-Y. Hu, S. Sun, H. Xu, and H. Sun, "Hybrid power-array rectenna with wide angle coverage for effectively harvesting RF energy of low power density," *IEEE Transactions on Microwave Theory and Techniques*, vol. 67, no. 1, pp. 402–413, 2019.

[73] Y.-Y. Hu, S. Sun, H.-J. Su, S. Yang, and J. Hu, "Dual-beam rectenna based on a short series-coupled patch array," *IEEE Transactions on Antennas and Propagation*, vol. 69, no. 9, pp. 5617–5630, 2021.

[74] M. Fantuzzi, G. Paolini, M. Shanawani, A. Costanzo, and D. Masotti, "An orientation-independent uhf rectenna array with a unified matching and decoupling rf network," *International Journal of Microwave and Wireless Technologies*, vol. 11, no. 5–6, p. 490–500, 2019.

[75] S. Roy, R. J.-J. Tiang, M. B. Roslee, M. T. Ahmed, and M. A. P. Mahmud, "Quad-band multiport rectenna for RF energy harvesting in ambient environment," *IEEE Access*, vol. 9, pp. 77464–77481, 2021.

[76] J.-M. Woo, W. Lim, J. Bae, C. M. Song, K.-J. Lee, S.-H. Yi, and Y. Yang, "Extendable array rectenna for a microwave wireless power transfer system," *IEEE Access*, vol. 9, pp. 98348–98360, 2021.

[77] M. Dinh, N. Ha-Van, N. T. Tung, and M. Thuy Le, "Dual-polarized wide-angle energy harvester for self-powered iot devices," *IEEE Access*, vol. 9, pp. 103376–103384, 2021.

[78] J. Liu, M. H. Zhang, S. T. Cai, and J. F. Chen, "A broadband rectifier with wide incident angle of incoming waves based on quadrature coupler for RF energy harvesting," *IEEE Microwave and Wireless Components Letters*, vol. 32, no. 12, pp. 1483–1486, 2022.

[79] M. Kumar, S. Kumar, and A. Sharma, "A compact 3-D multisector orientation insensitive wireless power transfer system," *IEEE Microwave and Wireless Components Letters*, pp. 1–4, 2022.

[80] D. Sood, M. Kumar, and J. Singh Ubhi, "A DC combining-free miniaturized mirror-like rectenna system with full-wave rectification for robust wireless power transfer in IoT at 2.45 GHz," *IEEE Microwave and Wireless Technology Letters*, vol. 35, no. 4, pp. 448–451, 2025.

[81] J. Liu, M. H. Zhang, and J. F. Chen, "A rectifier with less sensitivity to the incident angle of incoming waves based on quadrature coupler," *IEEE Transactions on Circuits and Systems II: Express Briefs*, vol. 70, no. 6, pp. 2261–2265, 2023.

[82] Z. Zhou, W. Lin, and Y.-X. Sun, "Wideband circularly polarized high-efficiency rectenna with large-angle wireless power capture capability," *IEEE Antennas and Wireless Propagation Letters*, vol. 23, no. 12, pp. 4428–4432, 2024.

[83] J. Huang, H. He, and H. Sun, "Robust-efficiency RF energy harvesting for internet of things applications," in *2019 Photonics & Electromagnetics Research Symposium - Fall (PIERS - Fall)*, pp. 314–317, 2019.

[84] S. Wang and H.-Y. Chang, "A 3d rectenna with all-polarization and omnidirectional capacity for IoT applications," in *2020 IEEE/MTT-S International Microwave Symposium (IMS)*, pp. 1188–1190, 2020.

[85] W. Shao, B. Yang, and N. Shinohara, "3-D printed multifocusing truncated gutman lens with high-efficient MMIC class-F load GaAs rectenna for mm-Wave battery-free IoT application," *IEEE Transactions on Components, Packaging and Manufacturing Technology*, vol. 14, no. 7, pp. 1319–1325, 2024.

[86] S. S. Vinnakota, R. Kumari, H. Meena, and B. Majumder, "Rectifier integrated multibeam luneburg lens employing artificial dielectric as a wireless power transfer medium at mm-wave band," *IEEE Photonics Journal*, vol. 13, no. 3, pp. 1–14, 2021.

[87] B. Majumder, S. S. Vinnakota, S. Upadhyay, and K. Kandasamy, "Dielectric metasurface inspired directional multi-port luneburg lens as a medium for 5g wireless power transfer—a design methodology," *IEEE Photonics Journal*, vol. 14, no. 3, pp. 1–10, 2022.

[88] F. Deng and K. M. Luk, "A broadband high-gain multibeam ambient millimeter-wave energy-harvesting system," *IEEE Internet of Things Journal*, vol. 11, no. 3, pp. 4888–4898, 2024.

[89] M. Joshi, K. Hu, C. A. Lynch, and M. M. Tentzeris, "Toward 5G wireless power harvesting: A promising broadbeam equiconvex lens-integrated mmWave harvester for smart city environments," *IEEE Microwave and Wireless Technology Letters*, vol. 35, no. 6, pp. 904–907, 2025.

[90] D. E. Brocker, J. P. Turpin, P. L. Werner, and D. H. Werner, "Optimization of gradient index lenses using quasi-conformal contour transformations,"

IEEE Antennas and Wireless Propagation Letters, vol. 13, pp. 1787–1791, 2014.

[91] W. Hu, C. M. Coco Martin, and D. Cavallo, "Design formulas for flat gradient index lenses with planar or spherical output wavefront," *IEEE Transactions on Antennas and Propagation*, vol. 72, no. 3, pp. 2555–2563, 2024.

[92] A. K. Baghel, S. S. Kulkarni, and S. K. Nayak, "Far-field wireless power transfer using grin lens metamaterial at ghz frequency," *IEEE Microwave and Wireless Components Letters*, vol. 29, no. 6, pp. 424–426, 2019.

[93] H. T. Ward, W. O. Puro, and D. M. Bowie, "Artificial dielectrics utilizing cylindrical and spherical voids," *Proceedings of the IRE*, vol. 44, no. 2, pp. 171–174, 1956.

[94] W. O. F. Carvalho, E. Moncada-Villa, and J. R. Mejía-Salazar, "Wireless at the nanoscale: Toward magnetically tunable beam steering," *IEEE Transactions on Antennas and Propagation*, vol. 71, no. 9, pp. 7473–7479, 2023.

[95] S. S. Vinnakota, R. Kumari, B. Majumder, and Q. H. Abbasi, "Numerical demonstration of a dispersion engineered metallic metasurface assisted mm-wave wireless sensor," *Opt. Continuum*, vol. 1, pp. 1795–1810, Aug 2022.

[96] B. Majumder, S. S. Vinnakota, M. K. Sreekavya, and B. Ghosh, "Microstrip fed all metal lens antenna - as a power transfer medium for 5g application," in *2023 IEEE Microwaves, Antennas, and Propagation Conference (MAPCON)*, pp. 1–5, 2023.

[97] W. Shao, B. Yang, N. Sakai, T. Hirai, K. Itoh, Q. Chen, and N. Shinohara, "Graded-index-fiber-inspired 3-d printed surface focusing porous dielectric structure with gaas mmic rectenna toward millimeter-wave wireless power transfer application," *IEEE Antennas and Wireless Propagation Letters*, vol. 22, no. 12, pp. 3177–3181, 2023.

[98] J. Shi, C. Song, Y. He, Q. Hua, B. Liu, J. Zheng, J. Zhang, S.-W. Wong, and Y. Huang, "Highly efficient asymmetric power division and system-level integration for millimeter-wave swipt: Theory, design, and experiment," *IEEE Transactions on Microwave Theory and Techniques*, pp. 1–17, 2025.

[99] S. Oh, D. H. Kim, W. Lee, J. Yang, C. Park, H. Lee, and S. K. Hong, "Millimeter-wave retrodirective wireless power transfer applicable to small electronic devices," *IEEE Journal of Microwaves*, vol. 5, no. 2, pp. 322–332, 2025.

[100] Y. Hu, F. Yang, L. Xu, Y. Wang, C. Zhang, and C. Song, "Flexible near-field communication in wearable electronics: Antenna design, measurements and system demonstration," *IEEE Journal of Selected Areas in Sensors*, pp. 1–10, 2025.

[101] F. Silva, P. Pinho, and N. B. Carvalho, "Multibeam beamforming technology in microwave power transfer and harvesting," *IEEE Journal of Microwaves*, vol. 5, no. 4, pp. 918–938, 2025.

[102] Y. Wang and W. Chen, "A novel design method of rf lens for long-range wireless power transmission," *IEEE Antennas and Wireless Propagation Letters*, vol. 16, pp. 3159–3162, 2017.

[103] J. Lee and S. Cho, "A 1.4-µw 24.9-ppm/°c current reference with process-insensitive temperature compensation in 0.18-µm cmos," *IEEE Journal of Solid-State Circuits*, vol. 47, no. 10, pp. 2527–2533, 2012.

[104] H. P. D. Paz, V. S. D. Silva, R. Diniz, R. Trevisoli, C. E. Capovilla, and I. R. S. Casella, "Temperature analysis of schottky diodes rectifiers for low-power rf energy harvesting applications," *IEEE Access*, vol. 11, pp. 54122–54132, 2023.

[105] J. Hagerty, F. Helmbrecht, W. McCalpin, R. Zane, and Z. Popovic, "Recycling ambient microwave energy with broad-band rectenna arrays," *IEEE Transactions on Microwave Theory and Techniques*, vol. 52, no. 3, pp. 1014–1024, 2004.

[106] X. Gu, J. Virgilio de Almeida, S. Hemour, R. Khazaka, and K. Wu, "Temperature-stable low-power rf-to-dc dickson charge pump rectifiers for battery-free sensing and iot systems," *IEEE Journal of Radio Frequency Identification*, vol. 8, pp. 632–642, 2024.

[107] Y. Wang, Y. Song, B. Zhang, S. Chen, Q. Chen, and C. Zhang, "A high-efficiency and reconfigurable rectenna array for dynamic output DC power control," *Frontiers in Physics*, vol. 10, p. 866656, 2022.

[108] J. Jing, L. Yan, B. Yang, P. Ren, J. Mi, C. Liu, and N. Shinohara, "Tailored and tunable microwave wireless power transfer for multiple targets in an electrically large cavity via frequency control," *IEEE Antennas and Wireless Propagation Letters*, pp. 1–5, 2025.

[109] Z. Liu, J. Wang, E. G. Lim, M. Leach, Z. Wang, R. Pei, Z. Jiang, W. Zhang, and Y. Huang, "Efficiency-enhanced wireless power transfer system featuring a pattern-reconfigurable antenna for mobile charging," *IEEE Antennas and Wireless Propagation Letters*, vol. 24, no. 11, pp. 4242–4246, 2025.

[110] Z. Zhu, B. Li, Y. Ke, Y. Wang, Z. Wang, S. Sun, P. Lu, F. Yang, C. Song, H. Dong, L. Zhang, and C. Zhang, "Adaptive radio frequency sensor enabled by electromechanically controlled stretchable rectifying antenna systems," *IEEE Open Journal of Antennas and Propagation*, vol. 5, no. 5, pp. 1229–1239, 2024.

[111] S. Shen, J. Kim, and B. Clerckx, "Closed-loop wireless power transfer with adaptive waveform and beamforming: Design, prototype, and experiment," *IEEE Journal of Microwaves*, vol. 3, no. 1, pp. 29–42, 2023.

[112] P. Lu, C. Song, F. Cheng, B. Zhang, and K. Huang, "A self-biased adaptive reconfigurable rectenna for microwave power transmission," *IEEE Transactions on Power Electronics*, vol. 35, no. 8, pp. 7749–7754, 2020.

[113] P. Lu, K. M. Huang, Y. Yang, F. Cheng, and L. Wu, "Frequency-reconfigurable rectenna with an adaptive matching stub for microwave power transmission," *IEEE Antennas and Wireless Propagation Letters*, vol. 18, no. 5, pp. 956–960, 2019.

[114] B. Clerckx and E. Bayguzina, "Low-complexity adaptive multisine waveform design for wireless power transfer," *IEEE Antennas and Wireless Propagation Letters*, vol. 16, pp. 2207–2210, 2017.

[115] V. Marian, C. Vollaire, J. Verdier, and B. Allard, "Potentials of an adaptive rectenna circuit," *IEEE Antennas and Wireless Propagation Letters*, vol. 10, pp. 1393–1396, 2011.

[116] A. Sidibe, A. Takacs, G. Loubet, and D. Dragomirescu, "Ultra-compact and high-efficiency rectenna for wireless sensing applications in concrete structure," in *2020 IEEE/MTT-S International Microwave Symposium (IMS)*, pp. 988–991, 2020.

[117] Y. Bian, J. Wang, Z. Tang, and W. Wu, "A differential rectenna with improved power utilization for simultaneous wireless information and power transfer," *IEEE Antennas and Wireless Propagation Letters*, vol. 24, no. 11, pp. 4237–4241, 2025.

[118] H. Takao, S. Kizuna, K. Sawada, M. Sudou, and M. Ishida, "Rf-powered silicon-mems microsensors for distributed and embedded sensing applications," in *2007 Fourth International Conference on Networked Sensing Systems*, pp. 35–42, 2007.

[119] Y. Wang, H. Pan, and T.-T. Chan, "A dual-band dual-sense circularly polarized rectenna for millimeter-wave power transmission," *IEEE Transactions on Antennas and Propagation*, vol. 73, no. 1, pp. 96–107, 2025.

[120] G. Moloudian, J. L. Buckley, and B. O'Flynn, "A novel rectenna with class-f harmonic structure for wireless power transfer," *IEEE Transactions on Circuits and Systems II: Express Briefs*, vol. 71, no. 2, pp. 617–621, 2024.

[121] J. M. Kovitz, M. Grady, J. Dee, C.-W. Chan, C. T. Rodenbeck, and C. R. Valenta, "Design and characterization of low-power rectifiers at x-band using a low-barrier schottky diode for wireless power transfer applications," in *2023 IEEE/MTT-S International Microwave Symposium - IMS 2023*, pp. 1006–1008, 2023.

ATHUL PARAMESWARAN (Graduate Student Member, IEEE) received the B.Tech. degree in Electronics and Communication Engineering from APJ Abdul Kalam Technological University, Kerala, India, in 2019. He was a Project Assistant at the Microwave Laboratory, Indian Institute of Science (IISc), Bangalore, from 2019 to 2021, working on the DoT-funded 5G Testbed Project with a focus on millimeter-wave active beam-steering antenna arrays. He is currently pursuing the Ph.D. degree at the Advanced Microwave Laboratory, Indian Institute of Space Science and Technology (IIST), Thiruvananthapuram, Kerala, where his research focuses on RF energy harvesting, high-efficiency Schottky rectifiers, adaptive matching networks, and self-powered IoT sensor nodes.

MANOJ KUMAR (MEMBER, IEEE) received the B.Tech. and M.Tech. degrees in electronics and communication engineering in 2016 and 2018, respectively, and the Ph.D. degree in electrical engineering from the Indian Institute of Technology Ropar, India, in 2023. He has industrial experience as an R&D Engineer at Perfect RFID, New Delhi, and as North India Sales Manager at Agmatel India Pvt. Ltd. Since March 2024, he has been a Postdoctoral Research Associate at the University of Glasgow, U.K., and is currently an INSPIRE Faculty with the Department of Electrical Engineering, Indian Institute of Technology Kanpur, India. His research interests include novel materials for future 6G technologies and additive manufacturing in materials engineering.

BASUDEV MAJUMDER (MEMBER, IEEE) received the Ph.D. degree in electrical engineering from the Indian Institute of Technology Bombay, Mumbai, India, in 2017. From August 2017 to December 2017, he was an Assistant Professor with the Birla Institute of Technology and Science, Pilani (BITS Pilani), Hyderabad Campus, India. In December 2017, he joined the Department of Avionics, Indian Institute of Space Science and Technology (IIST), Department of Space, Government of India, as an Assistant Professor, where he has been an Associate Professor since July 2022. His research contributions include leaky-wave antennas, metasurfaces, and high-impedance surfaces. His current research interests span RF and applied electromagnetics, microwave, and millimeter-wave circuit design. He received the INSPIRE Faculty Award from the Department of Science and Technology, Government of India, in 2017.

IGNACIO JULIO GARCIA ZUAZOLA completed a Ph.D. in Electronics (Antennas) in 2008 (viva in 2010) at the University of Kent, Canterbury, UK. He obtained an Executive MBA in Business (part-time program) in 2016 from Cardiff Metropolitan University, UK, a B.Eng. in Telecommunications Engineering in 2003 from Queen Mary, University of London, an HND in Telecommunications Engineering in 2000 from North West London College, University of Middlesex, and an FPII in Industrial Electronics in 1995 from the School of Chemistry & Electronics of Indautxu, Spain. He has academic experience and has been employed as a Research Associate (2004) at the University of Kent; Research Engineer, Grade 9/9 (2006) at the University of Wales, Swansea, UK; Research Associate (2008) at the University of Kent; Senior Research Fellow (2011) at the University of Deusto, Bilbao, Spain; Visiting Senior Research Fellow (2011) at the University of Leeds, UK; Research Associate (2014) at Loughborough University, UK; Representative of Spain (2015) at the London School of Commerce, UK; and Lecturer in Electronic Engineering (2018) at the University of Portsmouth, UK. He holds educational awards in Electricity, Pneumatics & Hydraulics, and Robotics, and possesses relevant industrial experience, having been employed by Babcock & Wilcox (1993), Iberdrola (1995), Telefónica (1997), Thyssen Elevators (1998), Cell Communications (2000), Nokia Bell Labs (2020), and Bilbao Ekintza – Bilbao City Council (2021). He was also engaged in an SME specializing in electrical wiring (1996). He was appointed Senior Lecturer (2022) and currently serves as Reader in Electronic Engineering (2024) at London Metropolitan University (London Met), UK. Included in *Marquis Who's Who in the World* (2010 edition), he has published in leading international journals such as *IEEE Transactions*, *IET Proceedings*, and *Electronics Letters*. His current research interests include business development, single-band and multiband miniature antennas, and the use of Electromagnetic Band-Gap (EBG) structures and Frequency-Selective Surfaces (FSS). He has led the antennas research line, supervised and mentored graduate and postgraduate students, and currently bids for research grants. He contributes to the teaching, scientific, technological, and business development of London Met by promoting and strengthening its branding, research, and innovation activities. He is a Member of the IET (MIET), a Senior Member of the IEEE (SMIEEE), and a Senior Fellow of the Higher Education Academy (SFHEA).

M. JALEEL AKHTAR (Fellow, IEEE) received the Ph.D. degree in Electrical Engineering from the Otto-von-Guericke University of Magdeburg, Magdeburg, Germany, in 2003. He was a Scientist with the Central Electronics Engineering Research Institute, Pilani, India, from 1994 to 1997, where he was involved in the design and development of high-power microwave devices. From 2003 to 2009, he was a Post-Doctoral Research Scientist and a Project Leader with the Karlsruhe Institute of Technology (KIT-FZK), Karlsruhe, Germany, where he primarily worked in the areas of industrial microwave technology. In 2009, he joined the Department of Electrical Engineering, Indian Institute of Technology Kanpur (IIT Kanpur), Kanpur, India, where he is currently a Chair Professor. He has supervised more than 25 Ph.D. candidates and over 90 masters' students for their theses. He has been the lead investigator of more than 15 projects in various domains of RF and microwave technology. He is presently leading a major project involving establishment of a world class fully accredited EMI/EMC Test Facility at IIT Kanpur, India. Dr. Akhtar has authored two books and four book chapters. He has authored or co-authored over 180 papers in various peer-reviewed international journals and over 250 papers in international conference proceedings. He holds three patents on planar RF sensors for various applications. His current research interests include metamaterial inspired RF sensors, microwave, mm-wave and THz imaging, metasurface based RF systems, RF energy harvesting, wireless power transfer and functional materials-based wideband microwave absorbers for stealth technology and EMI/EMC applications. Dr. Akhtar is the Fellow of IEEE, Fellow of the Indian National Academy of Engineering, and a Fellow of IETE. He is a recipient of the Excellence-in-Teaching Award (ETA) 2021 from IIT Kanpur, and the CST University Publication Award in 2009 from the CST AG, Darmstadt, Germany. He is elected Administrative Committee (AdCom) member of the IEEE Microwave Theory and Technology Society (MTT-S), and 2025 MTT-S Education Committee Chair. He was the General Co-Chair of IEEE MAPCON-2023, and the MTT-S International Microwave and RF Conference (IMaRC 2021). He served as an Associate Editor of the IEEE Sensors Journal during 2020-2023, and is currently serving as an Editor of the IETE Technical Review, the IETE Journal of Research, and SADHANA - Academy Proceedings in Engineering Journal.

MANISH KUMAR (Member, IEEE) received the Ph.D. degree in Electronics from Kurukshetra University, Kurukshetra and CSIR-CEERI, Pilani Rajasthan, India, in 2021. From October 2016 to June 2020, he was an Assistant Professor with the University Institute of Engineering and Technology, Kurukshetra University, Kurukshetra, India. In July 2020, he joined the Department of Research and Innovation, SKAU, kuirukshetra, India, as an Assistant Professor, In June 2023, he joined the Department of Electronics , Zakir Husain Delhi College, University of Delhi, India, as an Assistant Professor contribute to research in Artificial Intelligence Material Science.